

Thermoelectric Coolers: Progress, Challenges, and Opportunities

Wen-Yi Chen, Xiao-Lei Shi, Jin Zou, and Zhi-Gang Chen*

Owing to the free of noise, mechanical component, working fluid, and chemical reaction, thermoelectric cooling is regarded as a suitable solution to address the greenhouse emission for the broad cooling scenarios. Here, the significant progress of state-of-the-art thermoelectric coolers is comprehensively summarized and the related aspects of materials, fundamental design, heat sinks, and structures, are overviewed. Particularly, the usage of thermoelectric coolers in smart city, greenhouse, and personal and chip thermal management is highlighted. In the end, current challenges and future opportunities for further improvement of designs, performance, and applications of thermoelectric coolers are pointed out.

1. Introduction

As a typical sustainable technology, thermoelectrics (TEs) can realize the direct conversion between electricity and thermal energy, and provide the functions of cooling or heating by a reverse effect.^[1] Therefore, TEs can be an important supporting technology for energy harvesting, as well as a niche technology for power generation, which will be a complementary technique for other sustainable energy harvesting techniques such as solar, wind, and wave power.^[2,4] Particularly, thermoelectric coolers (TECs) based on the Peltier effect have exhibited advantages compared to conventional refrigeration driven by electric power, including free of noise, mechanical component, working fluid, and chemical reaction.^[5,6] These advantages enable TECs to have good durability without maintenance in the long term and be potentially used in wide applications.

Generally, the structure of TECs is based on a conventional TE device (TED),^[7] which is composed of thermoelectric n-p materials connected by conductive metals and covered by

substrates on their two sides,^[8] as illustrated in the center of **Figure 1**. With the rapid development of physics, chemical, materials science, and technology, both TE materials and TECs have exhibited significant progress.^[6,9] In addition to conventional bulk materials,^[1] many new-type TE materials such as superlattices,^[10–15] 2D thin/thick solid films,^[16–20] 1D nano/microfibers,^[21,22] and organic conducting polymers (CPs),^[23,24] have been developed and applied to TECs. TECs have been applied to much wider scenarios including space cooling,^[25–27] wearable/portable cooler for personal thermal management,^[22,28–33] processors and on-chip cooling,^[11,34–41] light-emitting diodes (LEDs),^[42–46] batteries and battery pack,^[47–51] solid/portable refrigerators,^[52–55] fresh water generators,^[56,57] medical and biological applications,^[58–60] and solar-panel-related cooling systems of the building,^[61–74] as displayed in **Figure 1**.


The cooling capacity of a TEC is normally evaluated by the coefficient of performance (COP), defined as^[20,77]

$$\text{COP} = \frac{T_c}{T_h - T_c} \times \frac{\sqrt{1 + ZT} - T_h/T_c}{\sqrt{1 + ZT} + 1} \quad (1)$$

in which the critical parameters are the temperatures of the hot (T_h) and cold (T_c) side of a TEC and the dimensionless figure-of-merit ZT of thermoelectric materials, defined as $ZT = S^2\sigma T/\kappa$,^[5,78] where S is the Seebeck coefficient, σ is the electrical conductivity, κ is the thermal conductivity, and T is the absolute temperature, respectively. Generally, a higher ZT indicates higher thermoelectric energy conversion efficiency of a specific material, and a higher ZT determines a higher COP,^[20] as plotted in **Figure 2a**. So far, the COP of a conventional vapor compressor can achieve ≈ 0.9 – 1.2 .^[79] The idea COP of TECs required ≈ 4.4 – 4.6 to achieve the same cooling performance through calculation of reversed Carnot cycles. However, the current maximum module COPs for single-stage and multistage thermoelectric modules can only achieve 0.67 and 0.72,^[79] respectively. The materials in TECs with $ZT \approx 1$ are only sufficient for commercial low-power cooling such as personal cooling and chip cooling.^[80] Therefore, it is of significance to design high-performance TE materials with high ZT s, especially at near-room temperatures since most of TECs functionalize at near-room temperatures.^[19,51,65,77,81,82] **Figure 2b** compares reported peak ZT s of bulk TE materials reported in recent years, including Bi_2Te_3 ,^[83] $\text{Bi}_{0.5}\text{Sb}_{1.5}\text{Te}_3$ (BST),^[84] SnTe ,^[85] Mg_3Sb_2 Zintl,^[86] Cu_2Se composites,^[87] GeTe ,^[88] half-Heusler,^[89] PbTe ,^[90] skutterudite,^[91] SnSe ,^[92] BiCuSeO ,^[93]

W.-Y. Chen, X.-L. Shi, J. Zou, Z.-G. Chen
School of Mechanical and Ming Engineering
The University of Queensland
Brisbane, Queensland 4072, Australia
E-mail: zhigang.chen@uq.edu.au

X.-L. Shi, Z.-G. Chen
Centre for Future Materials
University of Southern Queensland
Springfield Central, Queensland 4300, Australia
X.-L. Shi, Z.-G. Chen
School of Chemistry and Physics
Queensland University of Technology
Brisbane, Queensland 4000, Australia

 The ORCID identification number(s) for the author(s) of this article can be found under <https://doi.org/10.1002/smt.202101235>.

DOI: 10.1002/smt.202101235

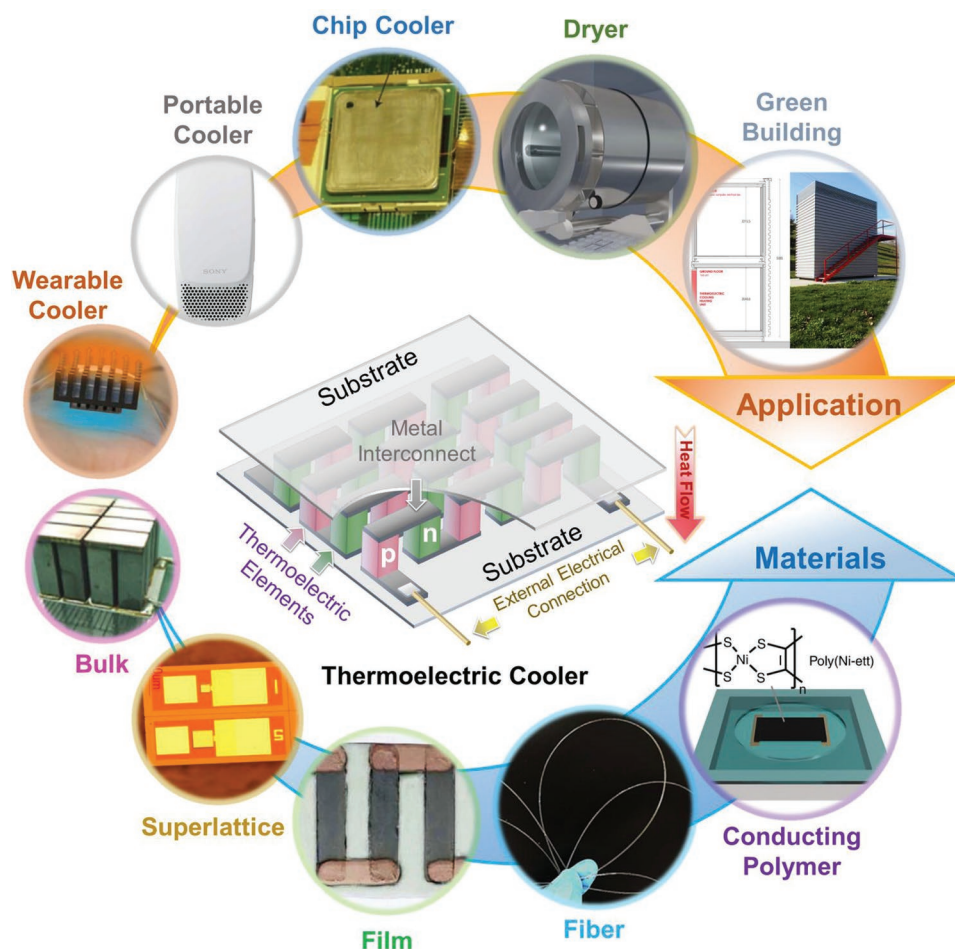


Figure 1. Structure, materials, and applications of thermoelectric coolers (TECs). Bulk; Reproduced with permission.^[75] Copyright 2017, Elsevier. Superlattice; Reproduced with permission.^[10] Copyright 2007, IEEE. Film; Reproduced with permission.^[16] Copyright 2016, Springer Nature. Fiber; Reproduced with permission.^[22] Copyright 2017, Elsevier. Conducting polymer; Reproduced under a Creative Commons Attribution 4.0 International License.^[23] Copyright 2018, the Author(s). Published by Springer Nature. Wearable Cooler; Reproduced under a Creative Commons Attribution 4.0 International License.^[31] Copyright 2019, the Author(s). Published by Springer Nature. Chip Cooler; Reproduced with permission.^[11] Copyright 2009, Springer Nature. Dryer; Reproduced with permission.^[76] Copyright 2018, Elsevier. Green building; Reproduced with permission.^[66] Copyright 2017, Elsevier.

and SrTiO_3 .^[94] Other TE materials such as Mg_2Si ($ZT = 1.4$ at 800 K),^[95] $\text{Cu}_2\text{S}_{1-x}\text{Te}_x$ ($ZT = 2.1$ at 1000 K),^[96] AgSbTe_2 ($ZT = 2.1$ at 573 K),^[97] and clathrate ($ZT = 1.45$ at 500 K),^[98] and also shows their high TE potentials. Noticeably, a record-high ZT of ≈ 3.1 was reported in oxide-removed Na-doped polycrystalline SnSe ,^[92] which was commented as breaking the thermoelectric performance limit.^[99] It should be noted that in addition to the temperatures and high ZT s, other parameters, such as the contact resistance between a TEC and heat sink,^[100] and internal and surface resistances of a TEC,^[101] also affect the whole cooling capacity in a real TEC system. Some reported maximum cooling performance ΔT_{max} and maximum COP (COP_{max}) of TECs based on bulk, film, and superlattice materials in recent 10 years are summarized in Figure 2c,d.^[11–13,16–18,20,22,23,25–27,30,32,33,35,36,38,40,52,53,56,57,61,62,73,102–115]

Till now, many articles have been overviewed the progress and challenges of thermoelectric cooling technology.^[8,50,63,65,77,82,116,121–130] These reviews contain both bulk and flexible structure, design, performance, and various applications. For example, a passive (phase change materials) and an active

(thermoelectric cooler) battery thermal management system and their limitations were overviewed,^[50] and a comprehensive review of solar thermoelectric cooling systems is reported.^[63] As well, the recent applications of TEs on medication were reviewed,^[131,132] as well as the progress on flexible TEs and their cooling applications.^[78,81,133] However, considering the recent rapid development of TECs, it is of great significance to maintain its up-to-the-date progress. In this work, we provide a targeted review of the progress, challenge, and outlooks of TECs based on their design, structures, fabrications, characteristics, performance, and broad application scenarios. We hope this review can benefit the future development of TECs with various purposes.

2. Fundamental of TEC

2.1. Materials and Structure

Materials used in TEC must possess high near-room-temperature ZT s. The most commonly used materials are

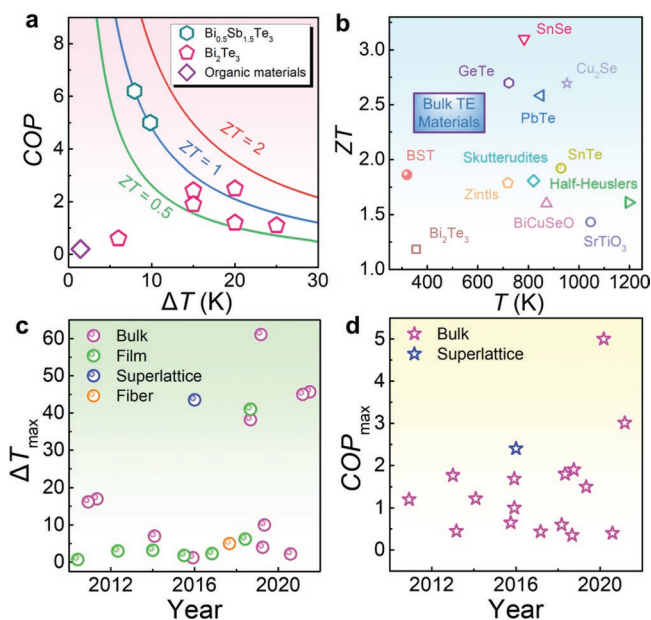


Figure 2. a) Relationship among the coefficient of performance (COP), the cooling performance ΔT , and the dimensionless figure-of-merit ZT . Thermoelectric coolers (TECs) with ZT s of materials are provided for comparison.^[20,22,23,57,61,116–120] b) Reported peak ZT s of state-of-the-art bulk TE materials.^[83–94] Timelines for c) maximum cooling performance ΔT_{max} and d) maximum COP (COP_{max}) of TECs based on bulk, film, and superlattice materials.^[11–13,16–18,20,22,23,25–27,30,32,33,35,36,38,40,52,53,56,57,61,62,73,102–115]

Bi₂Te₃ as n-type materials and BST as p-type materials, both with ZT s of >1 from 300 to 450 K, which are especially suitable for applying to TECs.^[12,83,84,134–138] The recently reported SnSe crystal with a room-temperature ZT of 1.25 is also attractive.^[102] In terms of the 2D TE materials that target to be employed in flexible TECs,^[19] n-type Bi₂Te₃-based thin film was reported to have a peak ZT of >1.6 at 300 K,^[139,140] and n-type Ag₂Se thin film exhibits a high ZT of 1.2 at 300 K.^[141] Correspondingly, p-type BST, Sb₂Te₃, and SrTiO₃ thin films show high ZT s of >1.5 at 300 K.^[142–144] Meanwhile, thin-film-based superlattices such as Bi₂Te₃/Sb₂Te₃ and PbSnSeTe/PbTe were reported to have high room-temperature ZT s of >2 ,^[12,145] indicating the full potential for applying to miniature TECs. Besides, 1D TE materials such as BST ($ZT = 1.25$)^[22] and SnSe ($ZT = 2$)^[146] fibers are also promising for applying to wearable TECs.^[28]

The conventional structure of TECs is similar to TE generators (TEGs), which are composed of a ceramic electrical insulator, p- and n-type TE elements (or legs), and electrodes to connect the TE elements.^[147] When current flows through n- and p-type semiconductors, a cold side is generated, and the other side becomes a hot side, which can be explained by the Peltier effect.^[148] As long as the cold side of TECs is attached to the heat source to absorb heat while dissipating the heat from the hot side, a cooling function can be easily generated.^[130] Generally, with increasing the current density, a higher ΔT can be achieved. However, the Joule heat and Thomson heat generated inside the TECs can become significant, which may cause unstable temperatures at both the cold and hot sides.^[147] Therefore, a heat sink is normally applied to the hot side to support the dissipation of the heat from TECs to ensure their stable ΔT s and COPs in most instances.^[100,149]

2.2. Heat Sink

The role of heat sinks is to maintain the stable temperature of the hot side of TECs and avoid overheating and damaging TECs at high ΔT .^[150] According to different application scenarios, there are different types of heat sinks, such as conventional fans and fins,^[79] heat pipes with phase change materials (PCMs),^[126] and flexible heat sinks.^[149] Figure 3a illustrates the fundamental principle of the heat sink, in which the cold side of TECs is attached to the heat source, while conventional fins are attached to the hot side of TECs. The heat is transferred from the cold side to the hot side and dissipated into the air-by-air convection. The heat sink enhances the air convection by increasing the contact area between the air and the hot end.^[150] However, since the fins are perpendicular to the airflow direction, the fins also hinder air convection, so the integration of fins and fans is considered a better choice than using one of them alone.^[150] Figure 3b is the photograph of a heat pipe, where the working principle is similar to the conventional combination of fins and fans. However, different from the fins and fans, heat pipes apply PCMs as the medium, including water and other liquid. Besides, heat pipes are regarded as to be more efficient than conventional heat sinks since the heat transfer medium has a higher specific heat capacity, which can take away more heat flux from the hot side.^[26] In addition to solid-state heat sinks discussed above, Figure 3c–d illustrates the typical structure and photo of flexible heat sinks fabricated by PCMs, copper foam, elastomer, metal foil.^[149] Such a flexible heat sink is a plurality of small-sized PCM blocks arranged on the elastomer, which can effectively support the wearable cooler to closely fit the human skin, contributing to stable ΔT on the TEC, as shown in Figure 3e.^[149] Meanwhile, the elastomer can increase the stretchability and durability of the heat sink since the bending force to PCMs can be offset by the elastomers.^[149] Figure 3f illustrates a wearable TE module with copper foams as the heat sink. Compared with conventional plate-fin heat sinks, the copper-foam heat sinks show better heat dissipation performance, which simultaneously improves the performance and flexibility of the TE module.^[151] Figure 3g illustrates the bending of the lightweight wearable TEC with a flexible heat sink composed of PCM/graphite/silicone elastomer.^[152] Such a ternary composite design can ensure high flexibility, high durability, and optimized heat capacity and thermal transport, which are key requirements for a heat sink to optimize the cooling performance of TECs and maintain a longer cooling capacity. The flexible heatsink is regarded as one of the most potent components of wearable TECs and self-power TEGs.

2.3. Design Rule

A design of a TEC aims to achieve a higher COP, which is closely related to the cooling capacity of the cold side (Q_c), optimum current (I_{opt}), and power input (P). According to the basic thermodynamic law of energy balance, Q_c can be defined as^[81]

$$Q_c = \Pi_{np} I - 0.5I^2 R - K(T_h - T_c) \quad (2)$$

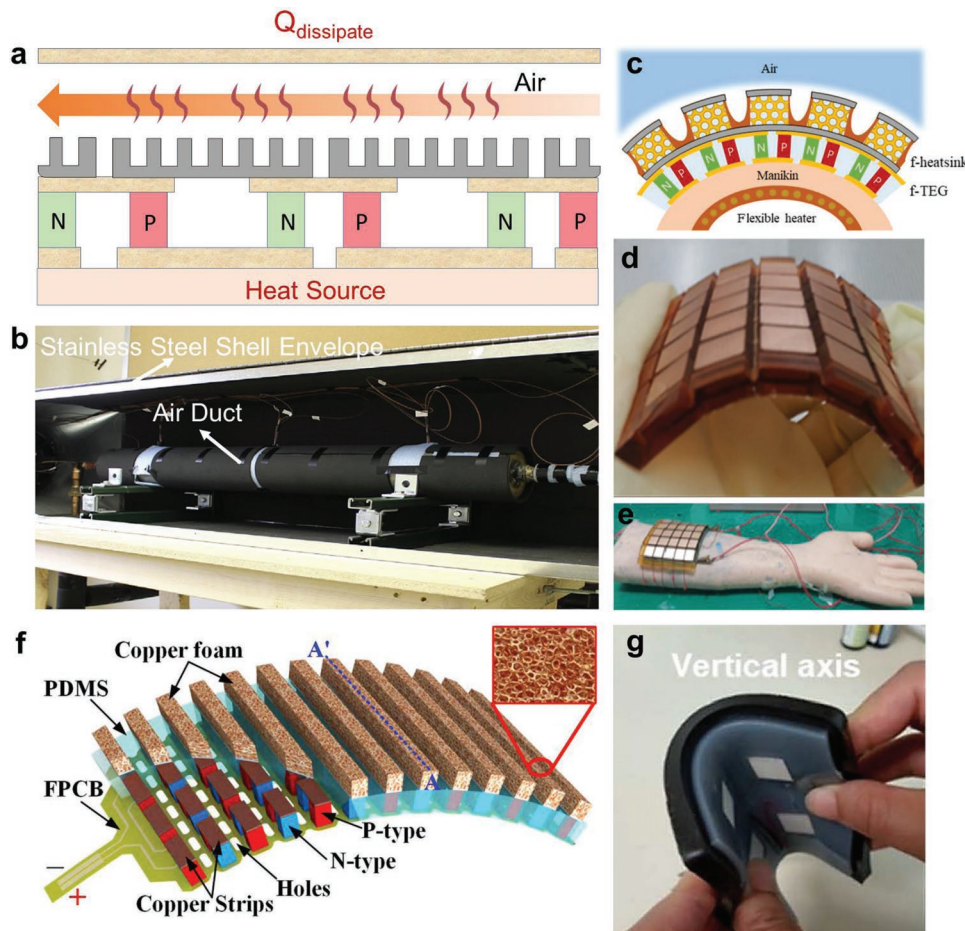


Figure 3. a) Illustration of the fundamental principle of heat sinks. Reproduced with permission.^[150] Copyright 2018, Elsevier. b) Photograph of the heat pipe. Reproduced with permission.^[26] Copyright 2014, Elsevier. c) Illustration of the flexible heat sink fabricated of phase change materials (PCMs), copper foam, elastomer, and metal foil. d) Photo of the flexible TEC with a flexible heat sink. e) Illustration of wearing the flexible thermoelectric cooler (TEC) with a flexible heat sink. Reproduced with permission.^[149] Copyright 2019, Elsevier. f) Illustration of a wearable TE module with copper foam as a heat sink. Reproduced with permission.^[151] Copyright 2018, IEEE. g) Illustration of bending the lightweight wearable TEC with flexible heat sink composed of PCM/graphite/silicone elastomer. Reproduced with permission.^[152] Copyright 2021, Royal Society of Chemistry.

where R is the electrical resistance, K is the thermal resistance, and Π_{np} is the Peltier coefficient of the TE module, in which R and K are highly related to the length (l) and cross-sectional area (A) of TE elements as well as their electrical resistivities (ρ) and κ ^[81]

$$R = \frac{l_n}{A_n} \rho_n + \frac{l_p}{A_p} \rho_p \quad (3)$$

$$K = \frac{A_n}{l_n} \kappa_n + \frac{A_p}{l_p} \kappa_p \quad (4)$$

A TEC needs an input electrical power to induce the Peltier cooling effect, so P is also critical when designing a TEC. P is closely related to the Seebeck voltage and current since ΔT of two sides is generated when P is applied to overcome the Seebeck voltage^[81]

$$P = S_{np} (T_h - T_c) I + I^2 R \quad (5)$$

Except for Q_c and P , appropriately applied current determines the performance of a TEC.^[34] Because the applied current can generate extra Joule heat by the internal electrical resistance when flowing through a TEC, the I_{opt} is required to minimize the impact of extra Joule heat on ΔT of the hot and cold sides,^[34] defined as^[34]

$$I_{opt} = \frac{(S_p - S_n)(T_h - T_c)}{R\sqrt{ZT_{avg} + 1} - 1} \quad (6)$$

where S_p and S_n are the Seebeck coefficients of p- and n-elements, and T_h and T_c are the hot- and cold-side temperatures. According to the equations above, Q_c , I_{opt} , and P are three interdependent parameters that can directly determine the COP of a TEC and avoid overheating caused by the extra Joule heat to damage the electrodes and materials.^[34] Furthermore, when considering the thermal cooling for electronic devices with a high heat source, the heat flux density (q) is also a referred parameter, which is the cooling power per unit area^[81]

$$q_{\max} = \frac{1}{l} \left\{ \left[\frac{1}{2} \frac{S_{sp}^2 T_c^2}{\rho} \right] - K(T_h - T_c) \right\} \quad (7)$$

The geometric parameter of the devices is another important factor for rationally designing a high-performance TEC.^[34] Generally, the thickness and length of components, electrodes, and ceramic electrical insulators need to be reasonably matched to ensure good thermal transport, which can avoid internal Joule heat and Thomson heat from affecting the cold-side temperature.^[34] The cross-sectional area of n- and p-type elements has a significant effect on the cooling performance of a TEC, especially for cooling within a short time since Joule heat is preferentially produced at the smaller cross-sectional area (Joule heat effect).^[153] A smaller cross-sectional area is considered more suitable as the hot side since the Joule heat is concentrated on the hot side, and the temperature of the cold side can be maintained for a longer time.^[153] Therefore, an appropriate area ratio of the hot and cold sides can effectively extend the cooling time and maintain a stable ΔT . The area ratio of the hot side to cold side is defined as^[153]

$$\gamma = \frac{A_{\text{semi,h}}}{A_{\text{semi,c}}} \quad (8)$$

where $A_{\text{semi,h}}$ and $A_{\text{semi,c}}$ are the cross-sectional areas of the hot and cold sides, respectively. Generally, the optimum ratio can be varied according to the difference of TE materials and applied current, so the ratio requires multiple tests during the design of a TEC.

The heat sink is an important part of designing a high-performance TEC since it is important to ensure a stable ΔT between the hot and cold sides, especially for applications with a relatively high-temperature heat source.^[34] When a heat sink is added to a TEC, some fundamental factors need to be considered, including the cross-sectional area and thickness of the heat sink, the thermal resistance of the heat sink, and the interface thermal resistance between the heat sink and the TEC.^[34] These factors are closely related to heat transfer.^[79] Moreover, the thermal transport of the heat sink affects the heat dissipation of the hot end of the TEC.^[34] Besides, some extra factors need to be considered according to the various types of heat sinks, as discussed in Section 2.2. Conventional fins are more related to the design structure, including the length and width of the fins,^[79] while heat pipe and exchanger are more focused on the choice of PCMs.^[150] Therefore, in addition to seeking a high-efficiency heat sink, a rational heat-sink design is highly needed, such as appropriate materials and structures which fit the application scenarios.

It should be noted that in addition to the interface thermal resistance between the heat sink and the TEC, expansion and contraction should also be considered since both can potentially damage the components. Although soldering or epoxying to the heat sink can achieve a better fit, this will produce a zero-tension point, which generally appears at the temperature where the solder or epoxy hardens and solidifies. If the TEC and the heat sink are cool back to room temperature, it may generate enough stress to damage the module. Therefore, it

is better to use thermal paste between the TEC and the heat sink, and use stainless steel screws to clamp them all together. This allows the components to “float” within the assembly. It is also necessary to use some physical retainers to prevent modules from leaving their original position because these parts expand and contract during working. Besides, although TECs mainly exhibit high mechanical strength in compression mode, their tensile and shear strengths are relatively low. Therefore, TECs should not be used to support the weight that withstands tension or shear stress. TECs should be moisture-free since moisture causes a decrease in cooling performance and corrosion of conductive materials. A rational gasketing material or other sealing systems that can block water vapor must be used, and the potting around the module can act as a secondary barrier to provide additional corrosion protection. Exposure to high temperatures should be avoided to extend the reliability of TECs. As the temperature rises, there is an increasing tendency for solder and copper to diffuse into the TE materials and destroy the cooling performance, and high temperatures may even cause the internal solder to melt. Furthermore, there are many parameters and conditions that affect the reliability of TECs, including module size and quality, assembly method, ambient temperature and humidity, temperature control system and technology, and temperature cycling. These factors can be rationally combined to produce a very low failure rate. Therefore, it is necessary to test the reliability of specific systems in applications where reliability is critical. Computationally assisted tools such as finite element analysis can be used to rationally design high-reliability TECs.^[119]

3. Fabrication and Performance of TEC

Commercial TEC is mainly based on commercial Bi_2Te_3 -based p- and n-type materials with a typical ZT of ≈ 0.7 at room temperature. **Table 1** shows typical technical features of a commercial TEC.^[104]

To explore a high ΔT and COP of a TEC, exploring high-performance and new-type TE materials is of significance to meet the requirement of broader application scenarios. Besides, rational structural designs of TEC and heat sinks are also vital for expanding their applications. Therefore, the recently reported TECs mainly focus on achieving high-performance, flexible/wearable, eco-friendly, and high cost-effective features to tackle more challenges in the future. From the material aspect, TECs with high performance still focus on conventional bulk materials. In terms of structures, both miniature and flexible TECs

Table 1. Specifications of a commercial TEC.^[104]

Specifications	Value
Maximum current (A)	8
Maximum voltage (V)	15.2
Maximum power (W)	80.3
ΔT_{\max} (K)	67
Dimensions ($L \times W \times H$) [mm]	$40 \times 40 \times 35$
Number of couples	127

are the main research directions to realize more functions such as on-chip cooling and personal thermal management. Besides, exploring low-cost fabrication processes, as well as boosting safety, are key issues that need to be solved. We carefully summarize current progress on materials, structures, properties, and applications of both commercial and new-type TECs in this chapter.^[11–13,16–18,20,22,23,25–27,30,32,33,35,36,38,40,52,53,56,57,61,62,73,102–115]

3.1. Bulk TEC

In terms of conventional bulk TECs, researchers mainly focus on improving their cooling performance and stability. To achieve this goal, many aspects such as the materials, structures, electrodes, and substrates are needed to be further improved to optimize their overall performance.^[9,81] Besides, a rational topological design such as fill factor and thermal resistance of the TE module should be considered since these factors may affect more than the ZT on the cooling performance,^[154] especially for the heat sources with high external thermal resistance such as human skin.^[31] Generally, the fill factor should be less than 15% while decreasing the ratio of length and width of TE legs to ensure the lower thermal resistance of TECs.^[31] As well, a rational topological design can considerably reduce the volume and cost of the devices and may achieve 1.7 times higher cooling performance than the conventional design of a TEC.^[31]

From a material aspect, because most of TECs work at near-room temperatures (250–400 K), till now, the best near-room-temperature bulk TE materials are p-type and n-type Bi_2Te_3 -based semiconductors,^[155] including p-type $\text{Bi}_{0.5}\text{Sb}_{1.5}\text{Te}_3$ ^[156] and Sb_2Te_3 ,^[157] and n-type Bi_2Te_3 and $\text{Bi}_2\text{Te}_{2.7}\text{Se}_{0.3}$.^[158] Figure 2b illustrates temperature-dependent ZT s of Bi_2Te_3 -based semiconductors. In which, n-type Bi_2Te_3 -based semiconductors can achieve high ZT s of >1.2 at near-room temperatures while p-type Bi_2Te_3 -based semiconductors exhibit even higher ZT s.^[12,83,84,134–138] High near-room temperature ZT s mainly come from their band structures with typical narrow bandgaps of 0.15–0.3 eV^[159] for ensuring high σ while the large band degeneracy is beneficial to achieve good S , contributing to high $S^2\sigma$.^[136] Meanwhile, Bi_2Te_3 -based semiconductor is a layer structure and consist of heavy atoms Bi and Te with natively low κ .^[160–162] Considering their near-room-temperature TE performance, Bi_2Te_3 -based semiconductors also act as inorganic “fillers” in inorganic/organic hybrid TE materials as flexible TECs.^[163]

In addition to improving the TE performance of Bi_2Te_3 -based semiconductors, TE researchers are also exploring alternative near-room-temperature TE materials with high performance because of the high cost of Bi_2Te_3 (especially for Te). Recently, a few promising near-room-temperature TE materials such as Ag_2Se ^[164–166] and SnSe ,^[102,167–169] were reported to have high near-room-temperature ZT s of >1 . For example, SnSe is a typical p-type semiconductor with a typical bandgap of ≈ 0.9 eV and an anisotropic layered structure.^[170–173] The high cost-effectiveness (without precious metals such as Ag),^[174] high intrinsic S of $>300 \mu\text{V K}^{-1}$,^[175–179] and ultralow intrinsic κ ^[180,181] make SnSe a promising candidate for employing in TECs. Besides, by rational doping and alloying with other compounds, high-performance n-type SnSe can be realized,^[182,183] but their

near-room-temperature ZT s are lower than their p-type counterparts.^[184,185] SnSe possesses a simple orthorhombic crystal structure but a complex electronic structure,^[148] which can be used as a guide to further improve its TE performance. Figure 4a shows multiband synglisis of Pb-doped p-type SnSe crystal by a combination of momentum and energy alignments.^[102] In this momentum alignment, the pudding-mold bands for the first two valence band maxima (VBM 1 and 2) merged into one band (VBM (1+2)), improving the carrier mobility μ and σ .^[102] The merged pudding-mold bands (VBM (1+2)) converge with VBM 3, enhancing the effective mass m^* and S .^[102] The bottom shows the Brillouin zone and Fermi surface with different Fermi levels. As a result, a high $S^2\sigma$ of $\approx 75 \mu\text{W cm}^{-1} \text{K}^{-2}$ and a high ZT of ≈ 1.25 were achieved at 300 K, and a high average ZT of ≈ 1.9 within the temperature range from 300 to 773 K was observed (Figure 2b).^[102] A TEC was assembled by using the developed $\text{Sn}_{0.91}\text{Pb}_{0.09}\text{Se}$ crystals and its ΔT_{max} is shown in Figure 4b.^[102] As can be seen, a high ΔT_{max} of ≈ 18 K can be achieved by the SnSe -based single-leg device, which is competitive to that of the conventional BST-based single-leg device.^[102] Figure 4c shows the ΔT_{max} of 31-pair TECs using $\text{Sn}_{0.91}\text{Pb}_{0.09}\text{Se}$ crystals and commercial BST as p-type legs and both using commercial $\text{Bi}_2\text{Te}_{2.7}\text{Se}_{0.3}$ as n-type legs. The inset optical image shows the as-fabricated device.^[102] A ΔT_{max} of ≈ 45.7 K can be achieved, indicating great potential for commercialization of SnSe -based TECs. In addition to SnSe crystals, polycrystalline SnSe was recently reported to exhibit a high peak ZT of ≈ 3.1 at 783 K and a record-high average ZT of ≈ 2.0 from 400 to 783 K,^[92] indicating potential for applying to the TECs working within this temperature range.

In addition to developing eco-friendly and cost-effective TE materials with high near-room-temperature TE performance, designs of TEC structures are also significant. For example, to realize a maximum TE conversion efficiency, multiple TE materials with different optimal performance temperature ranges are combined to form TE legs, which can be guided by computation-assisted tools.^[186] Besides, multistage-based structural design was proved to be effective for achieving high cooling efficiency. To achieve this goal, TE materials may need to be self-designed rather than directly using commercial materials. Figure 4d illustrates the fabrication of $\text{Bi}_x\text{Sb}_{2-x}\text{Te}_3$ ingots using a hot extrusion method, which can achieve sufficient mechanical properties for the construction of TECs.^[52] Figure 4e is a 3D view of a two-stage ultralow temperature TE module composed of $\text{Bi}_{0.91}\text{Sb}_{0.09}$ alloys as n-type legs and optimized $\text{Bi}_{1.6}\text{Sb}_{0.4}\text{Te}_3$ as p-type legs with different dimensions.^[52] Such a newly designed two-stage ultralow temperature TE module is integrated with an extra four-stage commercial TE module composed of n- and p-type Bi_2Te_3 -based alloys, giving rise to a ΔT_{max} of 45 K and a maximum cooling capacity Q_c of 85 mW, as shown in Figure 4f.^[52] Therefore, rational multistage design can be greatly beneficial to improve the performance of TECs.

Substrates and electrodes of TECs are crucial for achieving high cooling performance and high stability. Besides, rationally designing flexible substrates and electrodes can realize wearable TECs that are used for human body cooling. Figure 5a illustrates the structure of a flexible device, and Figure 5b shows its photo from a side view. Figure 5c illustrates the cooling garments with wearable TEDs, which are composed

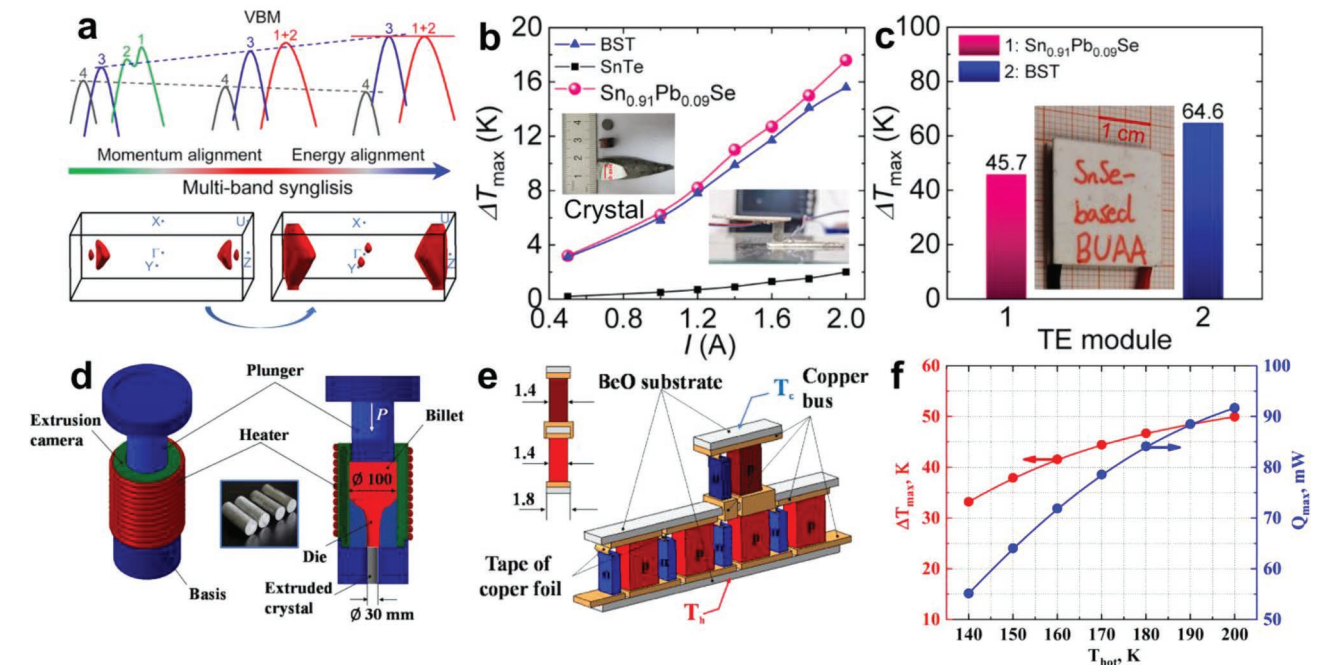


Figure 4. a) Multiband synglisis of Pb-doped p-type SnSe crystal by a combination of momentum and energy alignments. The bottom shows the Brillouin zone and Fermi surface with different Fermi levels. b) The maximum cooling performance ΔT_{\max} of the single-leg devices based on $\text{Sn}_{0.91}\text{Pb}_{0.09}\text{Se}$ crystals, commercial $\text{Bi}_{0.5}\text{Sb}_{1.5}\text{Te}_3$ (BST), and pure SnTe. The insets show optical images of $\text{Sn}_{0.91}\text{Pb}_{0.09}\text{Se}$ crystals and the as-fabricated single-leg device. c) ΔT_{\max} of 31-pair TECs using $\text{Sn}_{0.91}\text{Pb}_{0.09}\text{Se}$ crystals and commercial BST as p-type legs and both using commercial $\text{Bi}_2\text{Te}_{2.7}\text{Se}_{0.3}$ as n-type legs. The inset optical image shows the as-fabricated device. Reproduced with permission.^[102] Copyright 2021, American Association for the Advancement of Science. d) Illustrations of using hot extrusion technique to fabricate $\text{Bi}_x\text{Sb}_{2-x}\text{Te}_3$ ingots. e) 3D view of a two-stage ultralow temperature TE module. f) Corresponding ΔT_{\max} and maximum cooling capacity Q_{\max} as a function of hot temperature T_{hot} . Reproduced with permission.^[52] Copyright 2021, Elsevier.

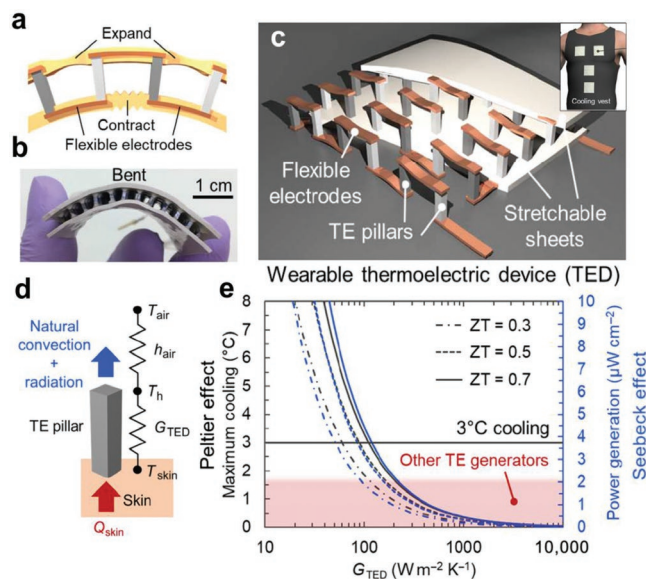


Figure 5. a) Schematic illustration of the structure and b) photo of the flexible thermoelectric device (TED). c) Schematic illustration of cooling garments with wearable TEDs. d) Schematic illustration of the geometry and thermal conditions for simulation. e) Cooling and power generation performance as functions of the thermal conductance of the TED (G_{TED}) and ZT. Simulation results are included for comparison. Reproduced with permission.^[33] Copyright 2019, American Association for the Advancement of Science (AAAS).

of conventional bulk TE legs and flexible substrates and electrodes.^[33] In such TEDs, the flexibility of TEC is mainly derived from the substrates composed of stretchable sheets and flexible electrodes. Figure 5d illustrates the geometry and thermal conditions for simulation,^[33] and Figure 5e shows the cooling and power generation performance as functions of the thermal conductance of the TED (G_{TED}) and ZT.^[33] The simulation results are included for comparison. Generally, a low G_{TED} that matches human metabolic heat, and natural convection conditions, are two prerequisites to achieve active cooling on human skin without a heat sink. With decreasing G_{TED} , both the cooling and power generation increase. When the ZT value of the TED is 0.7, a ΔT of >3 °C and a power generation density of >4 mW cm^{-2} can be achieved at G_{TED} of <120 W m^{-2} K^{-1} .^[33]

3.2. Film- and Fiber-Based TEC

In addition to 3D bulk TECs, 2D film-based TECs exhibit broader applications due to their higher portability and flexibility, even though their cooling performance is lower than that of conventional bulk TECs. With developing the fabrication technique of thin/thick films, their TE performance has been significantly improved. For example, at room temperature, n-type Bi_2Te_3 -based thin films were reported to have high ZTs of >2.2 and 1.6 ,^[139,140] n-type Ag_2Se thin film exhibited a high ZT of 1.2 ,^[141] and p-type BST, Sb_2Te_3 , and SrTiO_3 thin films showed high ZTs of >1.5 .^[142–144] A few fabrication

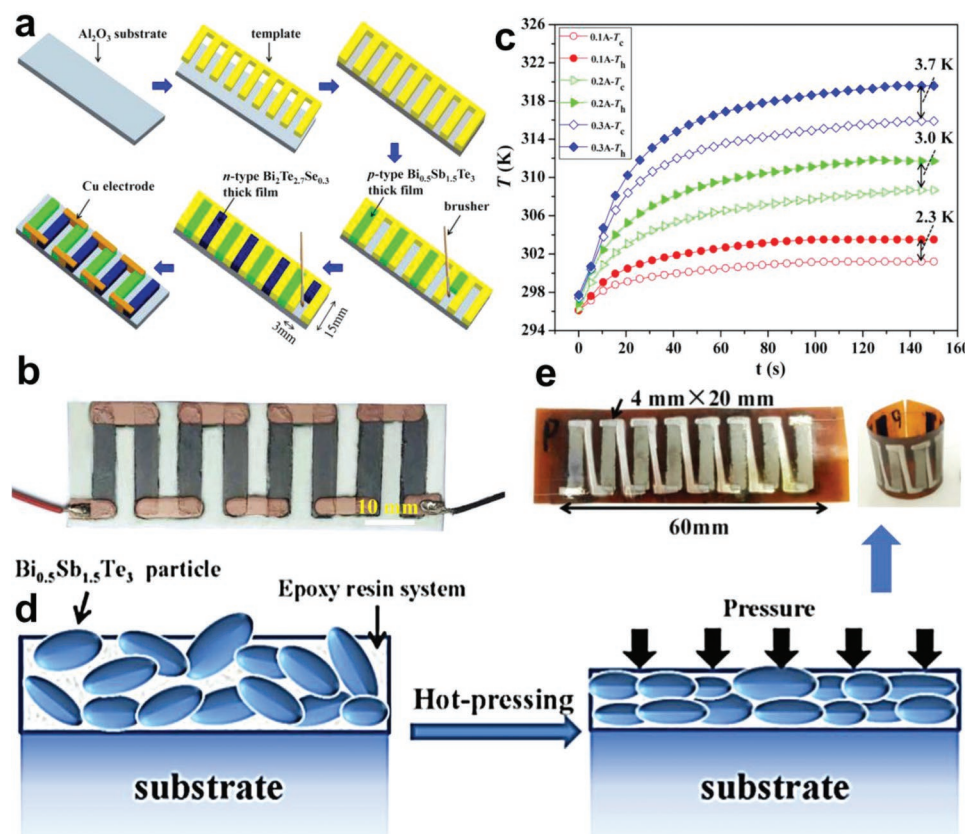


Figure 6. a) Schematic illustration of fabricating Bi₂Te₃-based thick films and devices by a brush printing method. b) Photo of the as-fabricated thick-film-based prototype device. c) Corresponding cooling performance. Reproduced with permission.^[16] Copyright 2017, Springer Nature. d) Schematic illustration of fabricating Bi_{0.5}Sb_{1.5}Te₃/epoxy thick films by a hot-pressing curing process. e) A prototype flexible device composed of thick films, Al/Cu/Ni multilayer thin-film electrodes, and a polyimide substrate. Reproduced with permission.^[20] Copyright 2018, Elsevier.

methods, such as solution method,^[187,188] spray pyrolysis,^[189] electrodeposition,^[190] pulsed laser deposition,^[191] chemical and electrochemical deposition,^[192] magnetron sputtering,^[143,193,194] flash evaporation,^[195] atomic layer deposition,^[196] hot wall epitaxy,^[197] thermal evaporation,^[198] brush plating,^[199] and bath deposition,^[200] have been used to fabricate TE films. **Figure 6a** illustrates the fabrication of Bi₂Te₃-based thick films and devices using a brush printing method.^[20] By using an Al₂O₃ substrate and a template, p-type Bi_{0.5}Sb_{1.5}Te₃ and n-type Bi₂Te_{2.7}Se_{0.3} thick films with 100–150 μm thickness are brush-printed on the substrate in sequence.^[20] A rational annealing process with a well-tuned annealing temperature (673 K for 4 h) plays an important role in promoting the densification of the films and preventing the films from cracking,^[20] which can achieve a relatively high $S^2\sigma$ of 1.5 μW cm⁻¹ K⁻² at 350 K. Figure 6b shows a photo of the thick-film-based prototype TEC device,^[16] and Figure 6c shows corresponding cooling performance. A ΔT_{\max} of ≈3.7 K can be achieved in the 4-paired TEC at a current of 0.3 A.^[16]

In addition to solid-state film-based TECs, flexible film-based TECs are also developed to meet the demand of applying TECs to wearable and round scenarios. Generally, there are two ways to realize the flexibility in film-based TECs, namely, fabricating inorganic or inorganic/organic hybrid films on an organic flexible substrate, and designing freestanding organic conducting polymer-based films.^[29,78,201] A film-based TEC composed of

p-type Bi_{0.5}Sb_{1.5}Te₃ and n-type Bi₂Te_{2.7}Se_{0.3} can be fabricated on a flexible polyimide substrate,^[109] which has a thickness of ≈5 μm and can achieve a ΔT_{\max} of 3.2 K.^[109] Figure 6d illustrates the fabrication of Bi_{0.5}Sb_{1.5}Te₃/epoxy thick films by a hot-pressing curing process, and Figure 6e shows a prototype flexible device composed of thick films, Al/Cu/Ni multilayer thin-film electrodes, and a polyimide substrate.^[20] Bi_{0.5}Sb_{1.5}Te₃ acts as TE components and epoxy resin acts as adhesive. By a hot-pressing process, a (0001) preferential orientation of Bi_{0.5}Sb_{1.5}Te₃ grains can be achieved, which gives rise to a high $S^2\sigma$ of 8.4 μW cm⁻¹ K⁻² at 300 K. A ΔT_{\max} of ≈6.2 K can be achieved in the 8-paired flexible TEC, at a current of 0.06 A.^[20]

In terms of the freestanding organic conducting polymer-based films, **Figure 7a** illustrates the molecular structure of poly(nickel-ethylenetetrathiolate) (Ni-ett) and the organic TED on the suspended 300 nm parylene film, and Figure 7b shows the corresponding optical image.^[23] Figure 7c shows the Peltier-effect-induced temperature distribution in the current direction at current densities of 0.3, 0.9, and 1.5 A mm⁻² for 0.01 s,^[23] indicating obvious Peltier effect in poly(Ni-ett). A ΔT_{\max} of ≈41 K can be achieved at the two contacts at a current density of 5 A mm⁻²,^[23] indicating great cooling potential in organic poly(Ni-ett) films.

In addition to 2D film-based flexible TECs, 1D flexible TE fibers and related wearable TECs are also developing.

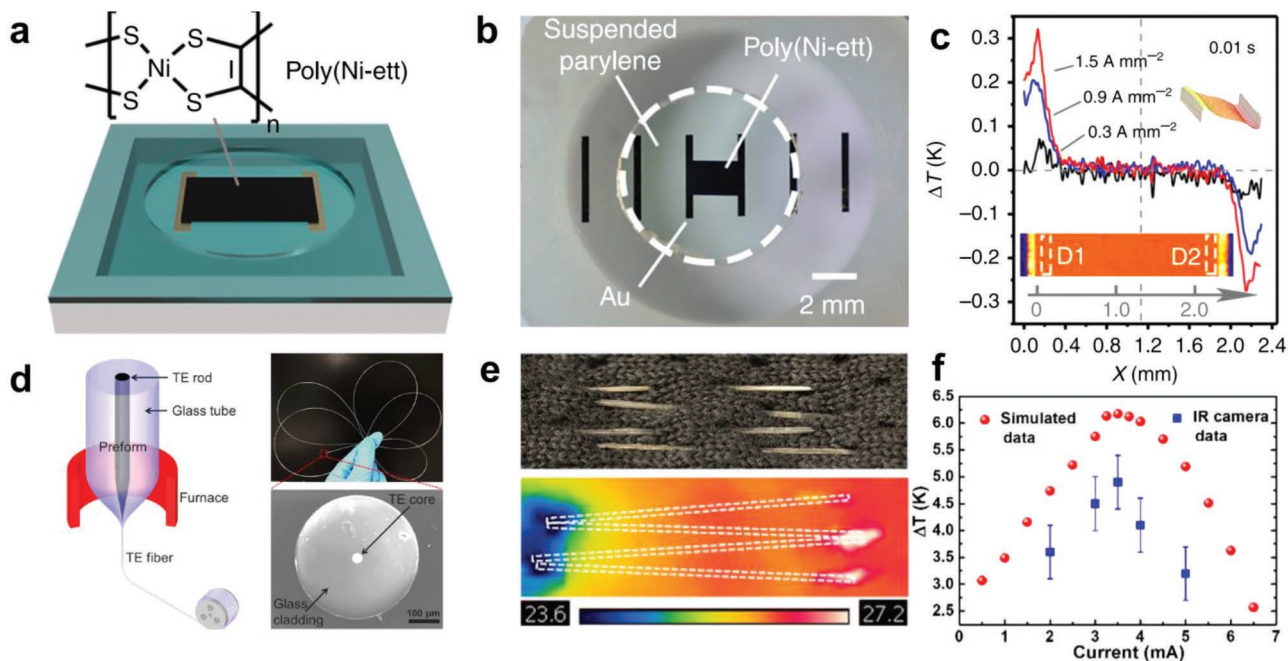


Figure 7. a) Schematic illustration of the molecular structure of poly(nickel-ethylenetetrathiolate) (Ni-ett) and the organic TED on the suspended parylene film. b) Corresponding optical image. c) Peltier-effect-induced temperature distribution in the current direction at current densities of 0.3, 0.9, and 1.5 A mm⁻² for 0.01 s. Reproduced with permission.^[23] Copyright 2018, Springer Nature. d) Illustration of fabricating p-type Bi_{0.5}Sb_{1.5}Te₃ and n-type Bi₂Se₃ flexible core-shell fibers. e) Infrared (IR) camera captured temperature profiles for the wearable cooling fabric with 2-pair p-n TE legs. The input current is 2 mA. f) Corresponding simulated and experimental ΔT . Reproduced with permission.^[22] Copyright 2017, Elsevier.

Compared to the film-based TECs, fiber-based TECs exhibit potentially higher flexibility and comfortability because of their 1D characteristics.^[21,28] There are various types of TE fibers, including carbon-based fibers such as carbon nanotubes,^[202,203] semiconductor-based fibers (freestanding and core-shell-structured),^[146,204] oxide-based fibers,^[205,206] coated glass fibers,^[207] CP-based organic fibers,^[208] and inorganic/organic hybrid fibers.^[209] Figure 7d illustrates the fabrication of p-type Bi_{0.5}Sb_{1.5}Te₃ and n-type Bi₂Se₃ flexible core-shell fibers by thermally drawing hermetically sealed high-quality inorganic TE materials in a flexible fiber-like substrate.^[22] The as-fabricated TE fibers are intrinsically crystalline, highly flexible, ultralong, and mechanically stable, which maintain the high TE properties as their bulk counterparts. Figure 7e shows infrared camera captured temperature profiles for the wearable cooling fabric with 2-pair p-n TE fiber legs.^[22] By an input current of 2 mA, a ΔT_{\max} of ≈ 5 K can be achieved,^[22] as shown in Figure 7f. The corresponding simulated data are provided for comparison.^[22] These results indicate that TE fibers and related TECs possess great potential for wearable applications such as personal cooling.

3.3. Superlattice-Based Device

Superlattice is a periodic structure of layers of normally two materials, and the thickness of each layer is several nanometers, such as Bi₂Te₃/Sb₂Te₃ (10/50 Å) superlattice as shown in Figure 8a.^[12] Such a structure has been proven to offer higher μ since the effect of interface scattering can be eliminated or

minimized,^[12] benefiting the high ZTs as reported.^[9,12] The superlattice structure has two main structures, which are parallel (in-plane) and perpendicular (cross-plane) to the film plane.^[14] The different structures apply different mechanisms to improve ZT.^[14] In-plane structures normally increase phonon interface scattering to reduce phonon thermal conductivity while applying quantum size effect to increase electron performance for higher ZT.^[14] Cross-plane structure has strong interfaces for reflecting phonons and also minimizing the interface scattering of electrons, together with electron energy filtering and thermionic emission to improve the electron performance for higher ZT.^[14] Therefore, superlattice-based TEDs, especially for miniature or micro-TECs,^[210] have been regarded as promising candidates for local cooling. It was reported that the p-type Sb₂Te₃/Bi₂Te₃-based superlattice has been successfully fabricated and can integrate into the on-chip cooler with an n-type δ -doped Bi₂Te_{3-x}Se_x.^[12,13] Figure 8b illustrates a Bi₂Te₃ superlattice-based TED and a scanning electron microscopy image of the as-fabricated superlattice, which was heteroepitaxially grown using metalorganic chemical vapor deposition.^[13] Figure 8c shows both experimental and predicted ΔT of TEC composed of p-type Sb₂Te₃/Bi₂Te₃ superlattice and n-type δ -doped Bi₂Te_{3-x}Se_x.^[13] By an input current of up to 15 A, a ΔT_{\max} of ≈ 45 K can be achieved.

Considering the high cost of electrical energy, multiple TE units can be designed and integrated. Figure 8d illustrates the fabrication of a 7 × 7 superlattice TE array, by which a ΔT_{\max} of 15 K can be achieved at a reduced current of 3 A.^[11] Each TE module is comprised of p- and n-type elements with Cu electrodes and AlN as the plates.^[11,13] Figure 8e shows measured

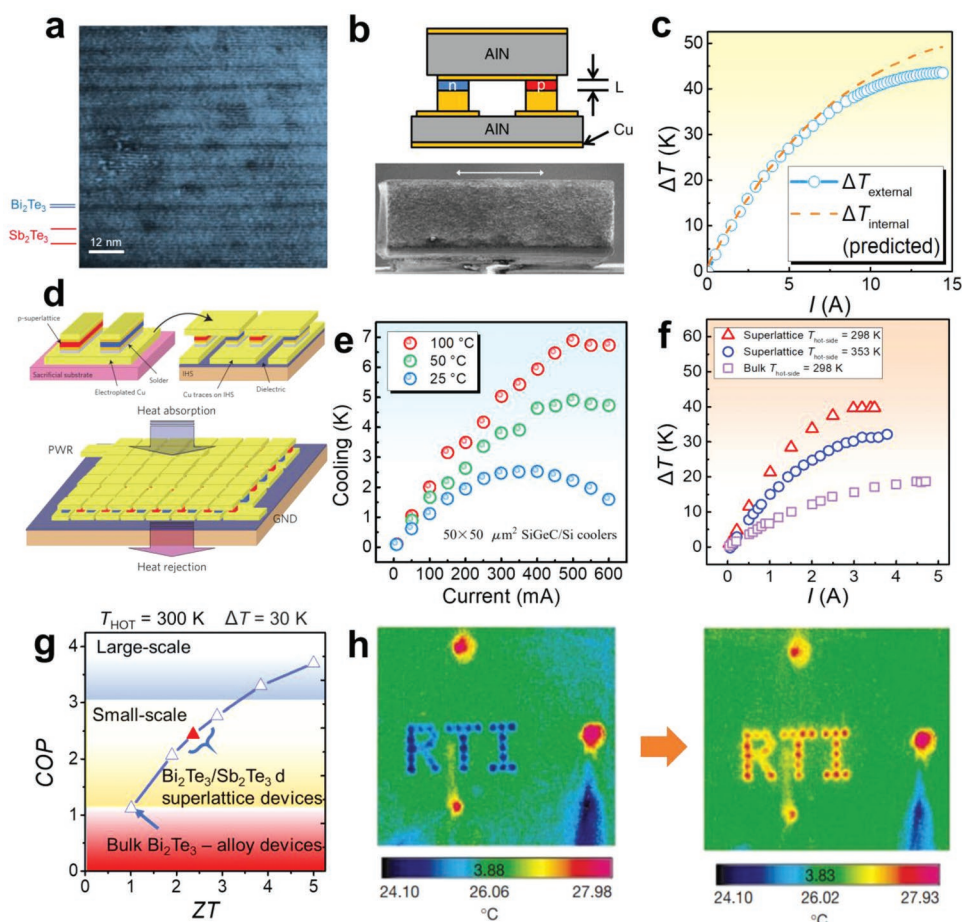


Figure 8. a) Transmission electron microscopy (TEM) image of a $\text{Bi}_2\text{Te}_3/\text{Sb}_2\text{Te}_3$ (10/50 Å) superlattice. Reproduced with permission.^[15] Copyright 1999, American Institute of Physics. b) Illustration of a Bi_2Te_3 superlattice-based TED and a scanning electron microscopy (SEM) image of the superlattice. c) Experimental and predicted ΔT of the thermoelectric cooler (TEC) composed of p-type $\text{Sb}_2\text{Te}_3/\text{Bi}_2\text{Te}_3$ superlattice and n-type δ -doped $\text{Bi}_2\text{Te}_{3-x}\text{Se}_x$. Reproduced under a Creative Commons Attribution 4.0 International License.^[13] Copyright 2016, the Author(s). Published by Springer Nature. d) Illustration of fabricating a 7×7 superlattice TE array. Reproduced with permission.^[11] Copyright 2009, Springer Nature. e) Measured ΔT s of $50 \times 50 \mu\text{m}^2$ SiGeC/Si superlattice-based TEC at various heat sink temperatures. Reproduced with permission.^[21] Copyright 2001, American Institute of Physics. f) Comparison of ΔT s of p-type $\text{Sb}_2\text{Te}_3/\text{Bi}_2\text{Te}_3$ conventional bulk and superlattice. g) The potential COP as a function of ZT in different scales of application. h) IR images of spots cooling/heating with p-type superlattice-based TEC. Reproduced with permission.^[12] Copyright 2001, Springer Nature.

ΔT s of $50 \times 50 \mu\text{m}^2$ SiGeC/Si superlattice-based TEC at various heat sink temperatures, in which a ΔT_{max} of ≈ 7 K can be achieved by a current of only 500 mA when the temperature of the heat sink is 100 °C.^[21] Figure 8f compares ΔT s of p-type $\text{Sb}_2\text{Te}_3/\text{Bi}_2\text{Te}_3$ conventional bulk and superlattice.^[12] ΔT s of superlattice-based TEC is much higher than that of conventional bulk-based TEC, while a higher hot-side temperature can further enhance ΔT . The ΔT s can achieve 32.2 and 40 K when the hot side is ≈ 298 and 353 K.^[12] In terms of the COP of superlattice-based TECs, Figure 8g shows potential COPs as a function of ZT in different scales of application.^[12] At a small scale, a COP of ≈ 2.5 can be achieved by $\text{Bi}_2\text{Te}_3/\text{Sb}_2\text{Te}_3$ superlattice-based TECs, owing to the high ZTs of superlattices (≈ 2.4 at 300 K).^[12] Figure 8h shows infrared images of spots cooling/heating with p-type superlattice-based TEC,^[12] which clearly show the cooling/heating effects by the devices.^[12] Therefore, superlattice-based TECs are promising candidates for small-scale cooling applications such as computer processors,

radio-frequency power devices, quantum cascade lasers, and DNA microarrays.^[13]

4. Application

With the rapid development of the TEC technique, the applications of TECs have successfully integrated into human life. Because of their characteristics such as low toxicity, free of noise, mechanical component, working fluid, and chemical reaction, and good durability without maintenance in the long term, TECs are especially suitable for cooling wearable and miniature electronics,^[30,32] central processing unit (CPU),^[35,37,40,41] LED light,^[43,46,107] dryer,^[76] refrigerator,^[54] battery pack,^[47,48,51,212] and even air conditioner.^[212] By further improving the performance and stability of TEC, it can be regarded as the main role in the field of biomedical,^[58] green building,^[74] and smart city.^[213]

4.1. Conventional Cooling

Conventional applications of TECs involve using commercial TECs composed of conventional Bi₂Te₃-based bulk materials. In other words, during conventional cooling, commercial TECs act as fixed components in the cooling system. Till now, based on various system designs, commercial TECs have been successfully employed in commercial products in the market, such as wine cabinets, mattresses, dehumidifiers, portable refrigerators, battery cabinets, cosmetic boxes, testing equipment, and instrumentation.

In addition to acting as fixed components in commercial products, commercial TECs can also be used for designing future products with huge market values. One concept for the application of commercial TECs is the green building with potential carbon neutrality, which is regarded as an important part of the smart city in the future.^[62] TECs are regarded as the most potential candidate for green building since the advantages of free CO₂ emission. **Figure 9a** illustrates the basic concept of the green building, in which a TEC-based ventilation system is driven by a concentrated photovoltaic CPV-TEG system. CPV-TEG is one of the most impressive drivers for the ventilation system in the green building and can effectively achieve zero-emission.^[74] For the working principle, PV panels are applied to absorb sunlight energy to transform into electric power by the PV effect, and then the generated electricity is supplied to the TE ventilation system. TE ventilation system is integrated by multiple parallel TECs and channel air ducts in each column, in which the supply air duct is close to the cold side of TECs to provide the cooling air. The dissipation air duct is close to the hot sides of TECs to discharge the excess heat generated from TECs. In winter, the ventilation system can also provide heating air with the converse direction of electric current. The whole ventilation system was predicted to only discharge about 29.6 kg CO₂, which is much lower than conventional fuel oil (411.42 kg), coal (540.71 kg), and natural gas (245.60 kg).^[74] Moreover, the system has been evaluated and able to have impressive performance. The efficiency of the ventilation system is highly related to the ZT values of the TE units, and the potential maximum COP can reach 4.17 at a ΔT of 20 °C.^[74] Such an outstanding performance suggests that the TEC may become the main research direction for the function of heating and cooling in the green building. Furthermore, by a combination of TECs, solar panels, heat exchange units, and electronic control units, a solar water condensation system can be built, which is self-powered and can be used in isolated and desert areas to condensate water from the surrounding humid air.^[129] However, compared with conventional water condensation methods, TEC-based systems may cost more electrical energy, which should be an issue that needs to be considered during application.

In addition to the green building and water condensation, conventional TECs can be integrated into large electronics such as air conditioners,^[212] refrigerators,^[54] and dryers.^[76] It was reported that an integrated model of TEGs, TECs, and battery packs has been developed for replacing the conventional air conditioner in vehicles. The TEGs absorb the waste heat from the engine and convert it into electric power and then collaborate with the battery pack to support the operation of TECs.^[212]

The evaluation of power consumption was conducted through the road test and proved that the TECs-based air conditioner can effectively reduce the power consumption by 45.8% compared with the traditional air conditioner.^[212] Except for the air conditioner, TECs can be integrated into the refrigerator to replace part of the traditional vapor compression components. **Figure 9b** shows the schematic diagram of a TEC employed in a refrigerator. Such a refrigerator is free of freon and working fluid, which can effectively reduce the emission of CO₂ and extend the cycle of maintenance. The hybrid refrigerators can effectively cool 17.5 kg of loads to the desired temperatures with lower noise, and the cooling time is 30–40% less than the conventional refrigerator with only vapor compression.^[54] Furthermore, the hot sides of TECs can also be used as heaters. In most recent, TECs are integrated as heat pump into the vapor compression dryers. Hybrid dryers can dry 2.95 kg of cloth with 6.51 lbc kW h⁻¹ and around 159 min.^[76] These results prove the function of TECs, although the efficiency of the hybrid dryer is still lower than a conventional dryer.

With the rapid development of the internet, most electronics and infrastructure have been able to connect to the internet and operation under the evaluation and analysis of the digital algorithms, therefore there are amounts of researches toward the smart TEC application due to its precise thermal management and efficient temperature response.^[213] It was reported that a TE-based air-conditioning (TE-AC) system smartly controlled by IoT can effectively improve the cooling capacity by 14% and COP by 46.3%.^[213] Similarly, the smart TECs can also be used for cooling server hosts since the increase of internet traffic and usage results in the amounts of heat, which can reduce the efficiency of the hosts. Lack of long-term precise temperature control can damage the server hosts and cause the interruption of the internet, leading to severe results in smart cities. Hence, TECs have been a critical part of smart cities in the future.

From the aspect of medical application, TECs are especially suitable for tissue cooling due to their advantages of lower energy consumption under a small temperature difference.^[59] Meanwhile, TECs can be applied to the cold wrapper for treating swelling and inflammation.^[58] The ability of precise temperature control and free of hazardous materials make TECs the most potential medical cooling implants. **Figure 9c** shows attaching self-designed TEC modules on the human body for localized cooling,^[31] which can cool the human skin up to 8.2 °C below the ambient temperature by combining effects of heat source/sink thermal resistances and properties of TE materials. Besides, it was reported that a cooling application based on integrating polydimethylsiloxane and TECs can treat the reversible brain deactivation in animals ranging from rodents to primates.^[59] The application can precisely fit the various geometry of the targeted cortical area, and the TECs can provide precise temperature control for supporting the mediating cessation of neural signaling in acute preparations of rodents, ferrets, and primates.^[59] A similar application was also reported for curing epilepsy and can cool the cortical surface to 22 °C in 30 s.^[214] The results further proved the sufficient good performance in the miniature TECs and the possibility of curing epilepsy as an implantable system for humans in the future.^[214] However, the relatively low COP and unknown effect on the brain function and histology of these applications

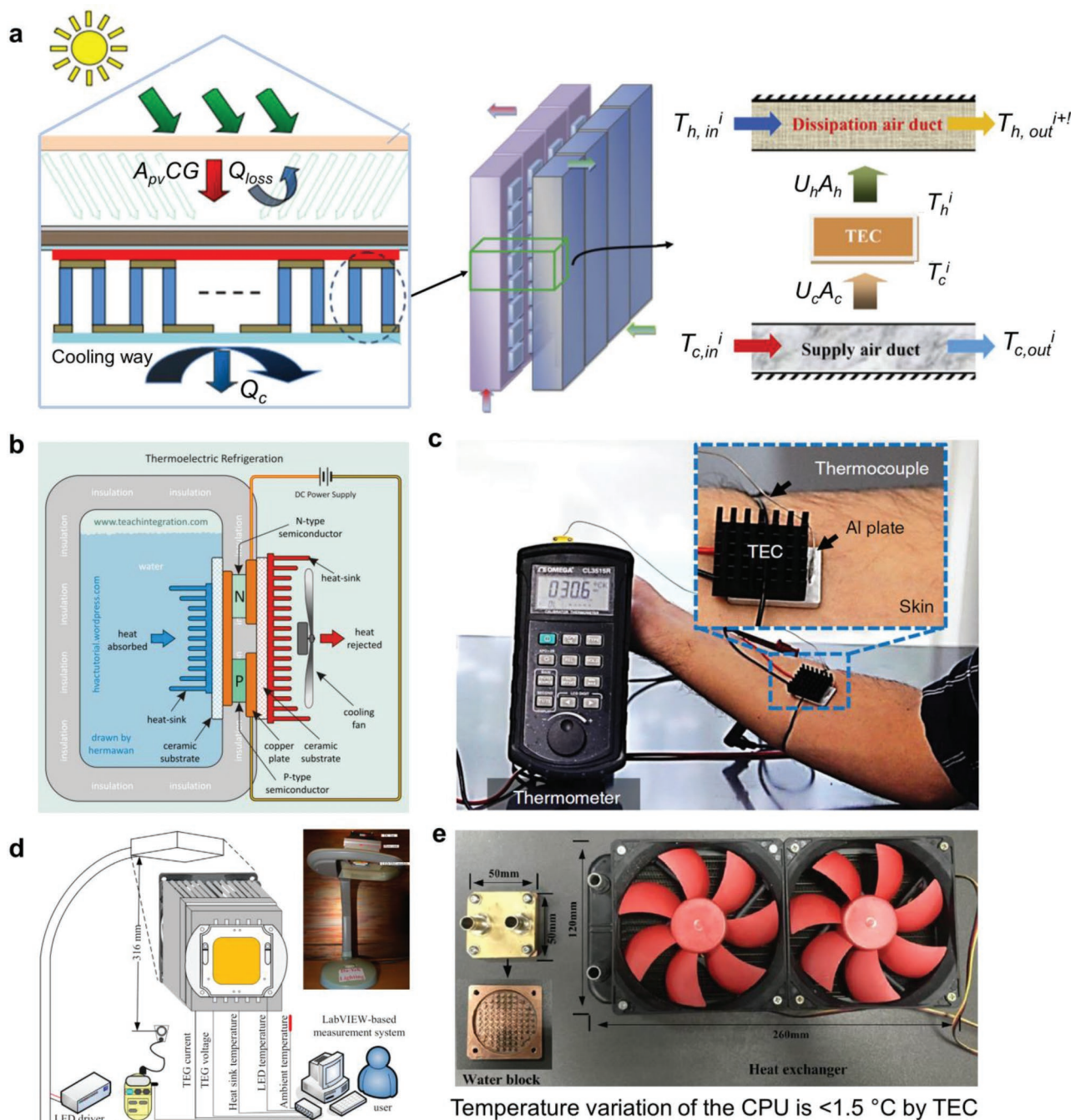


Figure 9. a) Schematic diagram of a thermoelectric cooler (TEC) based ventilation system driven by the concentrated photovoltaic-thermoelectric generators (CPV-TEG) for green building operations. Reproduced with permission.^[74] Copyright 2020, Elsevier. b) Schematic diagram of a thermoelectric cooler (TEC). Reproduced with permission from <https://hvactutorial.wordpress.com>. c) TEC modules on the human body for localized cooling. Reproduced under a Creative Commons Attribution 4.0 International License.^[31] Copyright 2019, the Author(s). Published by Springer Nature. d) Schematic diagram of an experimental test of active-cooling light emitter diode/TEC prototype by an automated measurement system. Reproduced with permission.^[44] Copyright 2016, Elsevier. e) CPU cooling using TEC with a water-cooled heat sink. Reproduced with permission.^[35] Copyright 2016, Elsevier.

are still the main challenges for the implanted devices and epilepsy cures. It should be noted that the requirements for using TEC-based devices in the human body are extreme, especially for implantable TECs since the human body is very sensitive to such implanted devices. Therefore, it may be relevant as a long-term vision for the mature application of implantable TECs. In

addition to the implants, TECs show potential to integrate with cryo-scalpel, medical cryogenic freezing mattresses, and bioreactor due to the precise temperature control, small size, and flexibility.

As discussed above, large-scale TECs mainly target greenhouses, large electronics, and industrial uses such as

communications, while medium-scale TECs mainly target personal, medical, and biological uses. In terms of small-scale TECs, commercial miniature TECs can be applied for locally cooling the LED lights and computer processors. For example, Figure 9d shows a schematic diagram of an experimental test of active-cooling LED/TEC prototype by an automated measurement system.^[44] Generally, LEDs requires more heat flux to provide higher light level according to daily usage, but the overheat of LEDs has become an issue. The cooling system that combines the TEC and corona wind cooling (CWC) was developed to solve this problem. It was reported that the well-coupled TEC and CWC can effectively maintain the temperature of LEDs below 80 °C.^[46] As well, two combinations containing TEC with the water-cooled microchannel heat sink (WMHS) and LED with the air-cooled heat sink were reported.^[43] TECs with WMHS have a higher performance of thermal management on LED, which can promise the temperature of LED below 60 °C, even though in the high-temperature environment.^[43] In addition to actively cooling LEDs, TECs can also efficiently cool processors. Figure 9e illustrates CPU cooling using TEC with a water-cooled heat sink.^[35] Similarly, an integrated TEC with a heat pipe as a heat sink can effectively cool the CPU by ≈15 K, proving that TECs can exhibit higher performance and lower cooling noise (below 40 dB) than the conventional cooling methods.^[37]

4.2. Personal Thermal Management

Personal thermal management (PTM) involves active personal cooling, heating, insulation, and thermoregulation, as illustrated in Figure 10a.^[215] Compared with traditional air/liquid cooling garments for the human body, TEC-based wearable and small electronics mainly focus on portable and wearable PTM, which can realize instant heating/cooling. Therefore, PTM is highly desirable for improving individual thermal comfort and reducing indoor heating, ventilation, and air conditioning (HVAC) energy consumption.^[32] Generally, commercial TECs can be conveniently integrated into other functional electronics to realize the functions of PTM. For example, Figure 10b shows a 3D structure of the TE energy conversion unit assembled with a control unit that contains a heating/cooling mode switch button and a rotary knob for air volume control,^[32] while Figure 10c illustrates the personal cooling and heating realized by the unit.^[32] In this PTM system, two heat sinks are installed on both sides of the TEC, which is composed of tens to hundreds of p–n elements. The duct flow provided by the blower on the supply side supplies air to the garment system, while the exhaust flow on the discharge side is used to accelerate heat transfer. The weight of the PTM system is <1 Kg, which is highly portable. Meanwhile, the as-designed PTM can provide the maximum personal cooling of 2.5 °C by a COP of >0.4 and personal heating of up to 5 °C, which can potentially save ≈15% HVAC energy without compromising thermal comfort. Similarly, it was reported that a portable TEC has been developed that can supply cool and warm air according to the demand of people.^[30] In most recent, Sony released a personal TEC that can be worn on the middle back below the neck, the cooling function is from the internal TE unit that can effectively cool

or heat the human body temperature (<https://reonpocket.sony.co.jp/>). It was reported that the Sony wearable cooler can cool body temperature around 5 K in summer and raise the body temperature around 7 K in winter.

To further improve the performance and comfortability of PTM, self-designed flexible TEDs can be integrated into PTM systems. Embedding the as-designed TEDs into the stretchable Ecoflex sheets can ensure a lower thermal resistance in the TEDs while having sufficient flexibility.^[33] The stretchable Ecoflex layer can support the bending of the human arm and closely adhere to the human skin, which promises comfortability and cooling efficiency, as shown in Figure 10d.^[33] Figure 10e is an IR image of the TED at hot-side temperature when worn on the human arm, which verifies that the heat energy is transferring from the human skin to the TED and dissipating to the environment.^[33] After removing the TED, the human skin shows a residual cooling effect, which can still induce 2.5 °C of cooling.^[33] The optimum current observed is lower than –80 mA, and can lead to a maximum cooling of >13 °C.^[33] In addition to indoor PTM, the as-designed flexible TEDs can be used for outdoor PTM. Figure 10f shows a schematic diagram of the TED armband integrated with the flexible battery pack for mobile thermoregulation.^[33] To investigate the effect of various convection and metabolic conditions, the device was tested under three realistic conditions, namely, sitting indoors, walking indoors, and walking outdoors under mild wind conditions, as shown in Figure 10g.^[33] The maximum cooling effect is 6 °C on the skin. During the ambient temperature varied from 22° to 36 °C, a comfort temperature of 32 °C can be maintained on the skin, indicating good outdoor PTM performance.

4.3. Chip Thermal Management

Chip thermal management (CTM) involves smart thermoregulation of chips based on active cooling and waste heat collection. A rationally designed CTM system can effectively maintain the chip at the optimal working temperature, maximize the working efficiency of the chip, and extend the service life of the chip. With the development of big data and 5G commercialization, 5G networks serve mobile phones, facilitate smart manufacturing factories, unmanned driving, and the Internet. However, the transmission capacity, transmission speed, and information processing speed will be more stringent than previous generations of communications, which put considerable pressure on maintaining the operations of 5G chips. The thermal management of 3G and 4G electronic products is relatively monotonous, and thermally conductive silicone sheets are generally used; while for 5G chips, the requirement of CTM has become tougher. In this situation, the TEC-based CTM system is a potential candidate to solve this issue.

Similar to PTM, commercial miniature TECs can be conveniently integrated into chips to realize the functions of CTM. For example, Figure 11a illustrates the temperature distribution in Compaq Alpha 21364 processor under executing a software load.^[41] It can be seen that there is a localized heat spot on the chip, therefore a special design of CTM structure is needed according to the size and heat distribution of targeted chips. Figure 11b illustrates a 5 × 5 TE module for on-chip cooling,

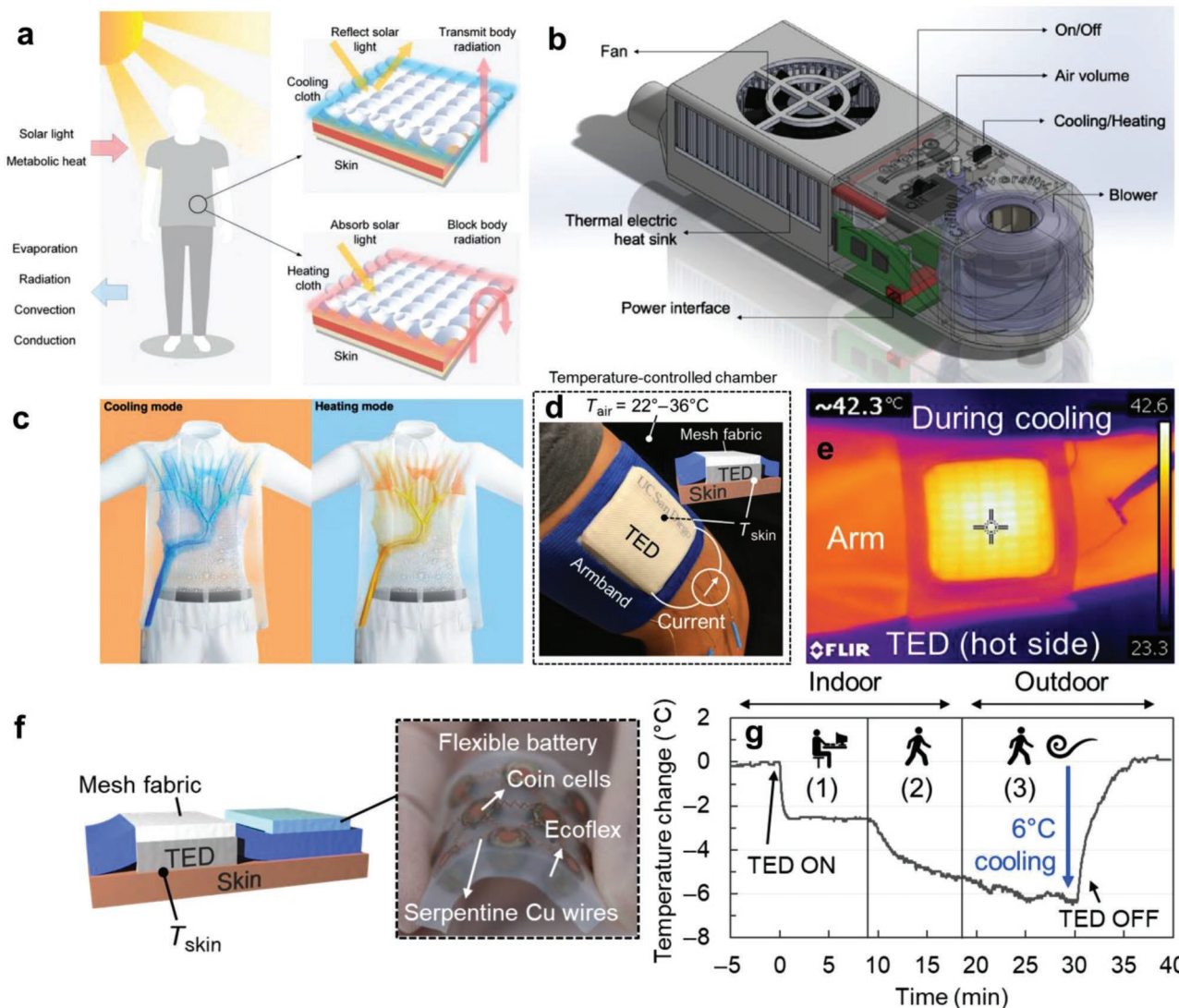


Figure 10. a) Schematic illustration of thermal analysis for personal thermal management (PTM). Reproduced with permission.^[215] Copyright 2020, Wiley-VCH GmbH. b) 3D structure of the thermoelectric energy conversion unit assembled with a control unit that contains a heating/cooling mode switch button and a rotary knob for air volume control. c) Illustration of the personal cooling and heating realized by the unit. Reproduced with permission.^[32] Copyright 2020, Elsevier. d) Schematic diagram of a TED armband. e) IR images of the TED armband (hot side) during cooling at current I of 160 mA on the arm. f) Schematic diagram of the TED armband integrated with the flexible battery pack. g) Skin temperature variation by TED cooling under three different conditions. Reproduced with permission.^[33] Copyright 2019, AAAS.

which can be composed by arrays of miniature commercial TEDs, as shown in Figure 11c.^[40] Figure 11d illustrates the TEDs act as both TEGs and TEC that cover on a $15 \times 15 \text{ mm}^2$ chip surface.^[40] One TED that acts as a TEC is covered on the heat spot of the chip, while the other TEDs act as TEGs to collect waste heat from the chip and convert it into electricity to power the TEC, forming a sustainable cooling system. Figure 11e,f exhibits temperature contours of the chip surface in the cases of “on” and “off” of the TEC-TEGs system.^[40] When the TEC-TEGs system is on, the harvested electrical energy by TEGs can power the TEC, leading to effective cooling of the whole surface of the target chip. Sometimes the dimensions of chips are very low, therefore commercial miniature TECs may be not

suitable for CTM. In these situations, self-designed TECs such as superlattice-based micro-TECs should be useful. Figure 11g illustrates the cross-section of the electronic test package with the Bi_2Te_3 superlattice-based TEC attached to the underside of the integrated heat spreader, while Figure 11h shows its photograph.^[11] Figure 11i shows an IR image of the test chip when only the localized heater is powered, illustrating the localized high heat flux that is to be cooled by the TEC.^[11] The chip is a typical silicon chip with a high heat flux of $\approx 1300 \text{ W cm}^{-2}$. The as-designed TEC can realize a $15 \text{ }^\circ\text{C}$ cooling performance during the chip work, indicating a promising CTM effect that can be widely used for CTMs of other scenarios such as insulated gate bipolar transistors and microbattery components in electronics.

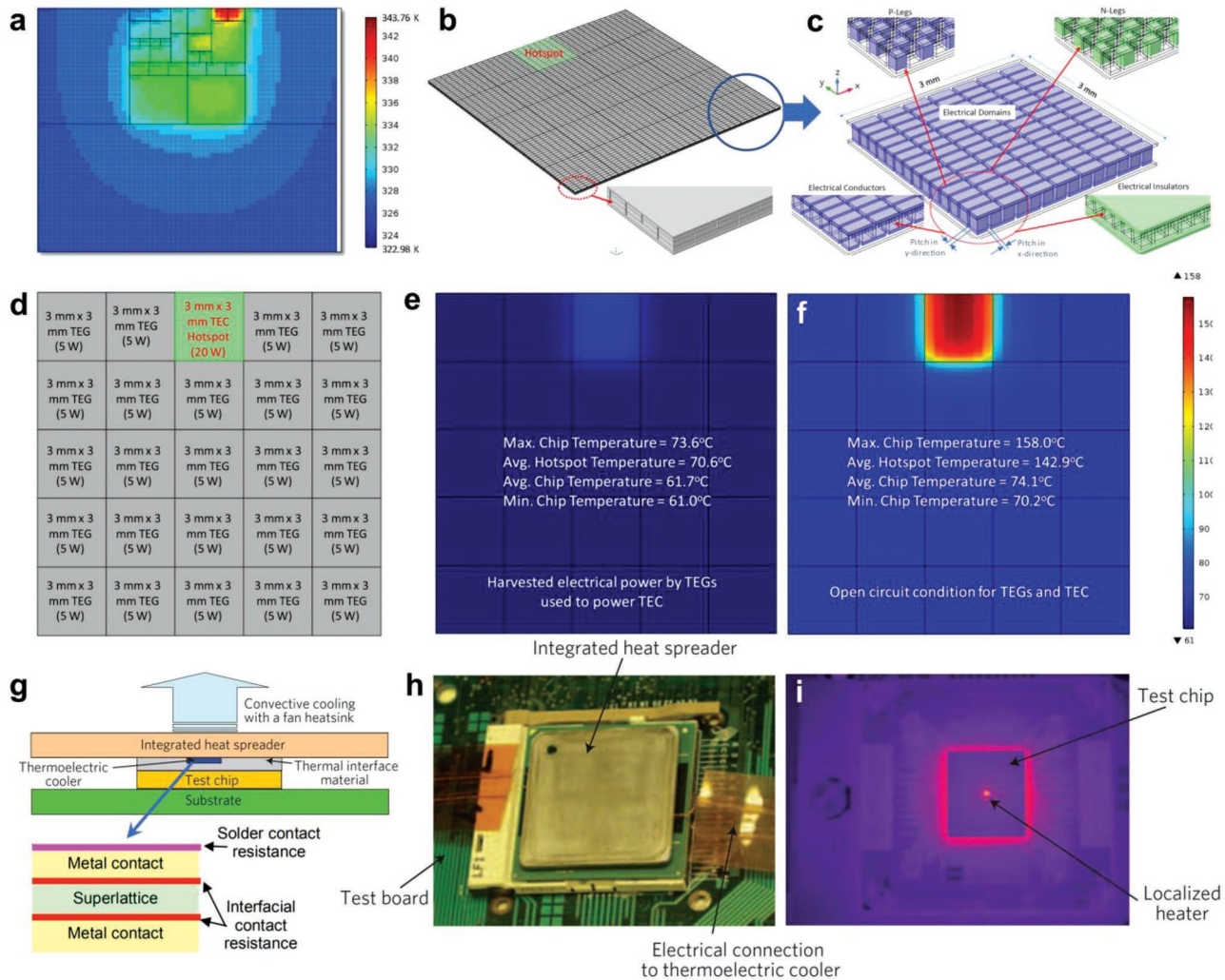


Figure 11. a) Temperature distribution in Compaq Alpha 21364 processor under executing a software load. Reproduced with permission.^[41] Copyright 2019, Elsevier. b) Illustration of a 5×5 thermoelectric module for on-chip cooling. c) Illustration of the structure of the thermoelectric module. d) Thermoelectric modules act as thermoelectric generators (TEGs) and thermoelectric coolers (TECs) that cover on a 15×15 mm² chip surface. Temperature contours of the chip surface in the cases of e) “on” and f) “off” of the TEC-TEGs system. Reproduced under a Creative Commons license.^[40] Copyright 2020, Elsevier. g) Illustration of the cross-section of the electronic test package with the superlattice-based TEC attached to the underside of the integrated heat spreader. h) Photograph of an electronic package with the TEC beneath the heat spreader. i) IR image of the test chip when only the localized heater is powered, illustrating the localized high heat flux that is to be cooled by the TEC. Reproduced with permission.^[11] Copyright 2009, Springer Nature.

5. Conclusion, Challenge, and Outlook

Benefiting from its irreplaceable flexibility, diversity, reliability, and many other advantages and characteristics, TECs have become key technologies that support many modern industries. From the viewpoint of commercialization, as a relatively mature solution, TECs can be widely used in consumer electronics, communications, medications, automobiles, industry, aerospace, oil and gas mining, and many other fields. In recent years, the research on high-performance, low-cost, eco-friendly, and multifunctional TECs has received extensive attention from researchers. The as-focused research objects involve almost all fields, such as military, science, aerospace, industry, agriculture, medical and health, biochemical, and daily necessities. PTM and CTM are two of the most promising research fields based

on flexible and miniature TECs, especially in the field of communications, high-performance micro-TECs have been a hot research topic by the rise of 5G network construction in 2019 since high-performance and high-reliability miniature TECs are especially promising solutions for temperature control of optical modules in 5G networks. The current research on TECs is still limited to TE materials, the maximum cooling capacity, and maximum cooling efficiency, while the heat-dissipation of the hot side has also been a research hot spot and difficult point of TECs. In addition to materials, researchers mainly focus on the research and development of module structural design and manufacturing, and system optimization. Therefore, the continuous research on new theory and new technology of TECs is of significance to tackle these issues, which are the main goals of current and future research of TECs.

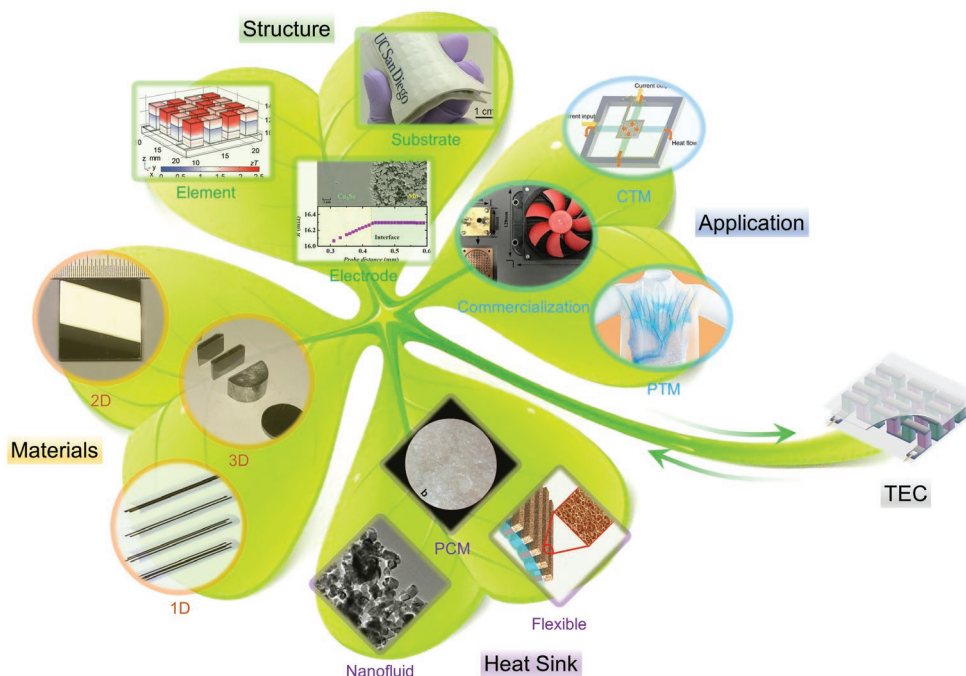


Figure 12. Outlooks of TECs based on four aspects, namely materials, structure, heat sink, and applications. For materials: 1D materials; Reproduced with permission.^[146] Copyright 2020, Wiley. 2D materials; Reproduced with permission.^[193] Copyright 2021, Elsevier. 3D materials; Reproduced with permission.^[180] Copyright 2019, Wiley. For structure: Element; Reproduced with permission.^[186] Copyright 2020, Royal Society of Chemistry. Substrate; Reproduced with permission.^[33] Copyright 2019, AAAS. Electrode; Reproduced with permission.^[216] Copyright 2019, Elsevier. For heat sink: PCM; Reproduced with permission.^[217] Copyright 2020, Elsevier. Nanofluid; Reproduced with permission.^[42] Copyright 2020, Elsevier. Flexible; Reproduced with permission.^[151] Copyright 2018, IEEE. For application: Commercialization; Reproduced with permission.^[35] Copyright 2016, Elsevier. CTM (chip thermal management); Reproduced with permission.^[218] Copyright 2018, Elsevier. PTM (personal thermal management); Reproduced with permission.^[32] Copyright 2020, Elsevier.

It should be noted that there is still a considerable challenge in developing TECs. The research of TECs involves the principle of heat transfer, the laws of thermodynamics and the Peltier effect, and many other factors such as the ZT of the material, the multistage structure, the optimal design of the cold and hot sides, etc. These various factors are complementary to each other, therefore the research of TECs has always faced many difficulties. First of all, the performance of TEC materials depends on their ZT values, but the three key parameters (σ , S , and κ) that determine the ZT are all functions of temperature, and are strongly coupled together. Meanwhile, ZT is sensitively dependent on the material type, composition, doping level, and micro/nanostructure. It is difficult to achieve high near-room-temperature ZT by simultaneously optimizing $S^2\sigma$ and suppressing κ . Therefore, the research of high ZT has always been a challenge in the research of TECs. Second, TECs are systematic processing with many parameters and complex changes in operating conditions. Geometrical structure parameters, as well as heat dissipation and heat transfer, have a great influence on the final performance of TECs. It is difficult to meet various needs by conventional experimental methods. During designs of TECs, different working conditions should be comprehensively considered to determine the best solution. Furthermore, according to the principle of heat transfer and the laws of thermodynamics and the Peltier effect, the temperature difference between the cold and hot sides of TECs has a great influence on the heat and cold transfer of TECs. Poor heat transfer per-

formance at both sides will greatly reduce the cooling capacity under the same power, which cannot meet the requirement for practical application. Therefore, increasing the heat dissipation of the cold and hot sides has become an issue. In conclusion, the difficulties of a rational TEC design involve developing TEC materials with high ZT s, interrelated parameters, and the design of heat dissipation at the hot and cold sides.

In terms of the outlooks for the future development of TECs, we summarize the following key points, which are schematically illustrated in **Figure 12**.^[33,42,146,151,180,186,193,216–218]

1. Investigating advanced materials. The near-room-temperature ZT s of current BST-based TE materials need to be further improved by rational compositional and structural designs while exploring new-type alternative high-performance near-room-temperature TE materials is also important to further reduce the cost and improve the mechanical stability of both materials and TECs. Computational assisted approaches are useful for designing new TEC materials or improving the TE performance of current TEC materials. Besides, in addition to developing bulk-based TEC materials, other types of materials such as 1D fibers, 2D thin/thick films and superlattices, CPs, and organic/inorganic hybrids also exhibit characterizations to be potentially employed in flexible/wearable and miniature TECs that target broader applications.
2. Novel design of heat sinks. To achieve better cooling performance, the dimensions and materials of conventional metal

fin-based heat sinks should be further perfected. Meanwhile, to achieve higher thermal dissipation ability, new-type heat sinks such as PCMs and flexible inorganic/organic foams are promising alternatives that target different application scenarios. Besides, in addition to water and fan that act as traditional cooling mediums, novel medium such as nanofluid is also valuable to be explored. Furthermore, good adhesion between the heat sinks and TE modules is critical for ensuring high reliability of the TEC. Therefore, designs of joints and adhesion between the base plates and TE module require to be further explored to increase the reliability and service life of TECs.

- Advanced structure and fabrication technique. Till now, TECs have been developed with different types that target various application scenarios, including conventional solid-state bulk-based TECs, thin-film- and fiber-based flexible TECs, and superlattice-based miniature and micro-TECs. However, regardless of the TEC type, a reasonable device structural design and system optimization are required to maintain stable cooling performance. Till now, there are few studies on the optimal design of the cooling system at the hot and cold sides, and the design of TEC is mostly at the stage of theoretical calculation. It is necessary to continuously in-depth research on the design of TEC modules and the optimization of system performance. With the rapid development of science and technology, the size of the target that needs to be cooled is either becoming larger or becoming smaller, and some targets are becoming increasingly complicated, therefore multiple factors need to be considered during a device structural design, such as filling factor, a combination of different TE materials, electrode materials, new sealants and welding technique, and solid/flexible substrates. Oxidization and moisture-proof are also needed to be considered when applying TECs to some harsh environments. TEC is a typical interdisciplinary subject that requires different aspects of knowledge to cooperate and make progress together.
- Expanding applications of TECs. Goals of developing advanced TECs are to apply them to scenarios that need solid-state cooling without noise and toxicity. According to the report data of MarketsandMarkets (<https://www.marketsandmarkets.com>), from 2017 to 2019, the market of TE system was 399 million U.S. dollars, 426 million U.S. dollars, and 460 million U.S. dollars, respectively, and it is expected to reach 741 million U.S. dollars in 2025. Most of which target consumer electronics and communications markets. In addition to these markets, TECs can be potentially widely used in many other fields. In the medical field, TECs can be used for precise temperature control of various instruments in laboratories such as cold compress equipment, portable insulin boxes, portable medicine boxes, and PCR testers. In the automotive field, TECs can be used for vehicle refrigerators, thermostat cup holders, thermostat seats, and thermal management of human-computer interaction systems, power batteries, and sensors. In the industrial field, TECs can be used for precise temperature control of flue gas cooling, charge-coupled device image sensors, laser diodes, and dew point testers. In the field of aerospace defense, TECs can be used for temperature control of detectors and sensors, cooling of laser systems, temperature adjustment of flight suits,

and cooling of equipment casings. Generally, the field of consumer electronics is the main practical application direction of TECs, while the communication field is the key development direction in the future.

Acknowledgements

W.-Y.C. and X.-L.S. contributed equally to this work. This work was financially supported by the Australian Research Council and Innovation Centre for Sustainable Steel Project.

Conflict of Interest

The authors declare no conflict of interest.

Keywords

application, coolers, devices, materials, thermoelectrics

Received: October 4, 2021

Revised: November 27, 2021

Published online: January 5, 2022

- G. Tan, L. D. Zhao, M. G. Kanatzidis, *Chem. Rev.* **2016**, *116*, 12123.
- S. Roychowdhury, T. Ghosh, R. Arora, M. Samanta, L. Xie, N. K. Singh, A. Soni, J. He, U. V. Waghmare, K. Biswas, *Science* **2021**, *371*, 722.
- Y. Zheng, T. J. Slade, L. Hu, X. Y. Tan, Y. Luo, Z.-Z. Luo, J. Xu, Q. Yan, M. G. Kanatzidis, *Chem. Soc. Rev.* **2021**, *50*, 9022.
- B. Jiang, Y. Yu, J. Cui, X. Liu, L. Xie, J. Liao, Q. Zhang, Y. Huang, S. Ning, B. Jia, B. Zhu, S. Bai, L. Chen, S. J. Pennycook, J. He, *Science* **2021**, *371*, 830.
- Y. Xiao, L.-D. Zhao, *Science* **2020**, *367*, 1196.
- X. Shi, L. Chen, *Nat. Mater.* **2016**, *15*, 691.
- G. J. Snyder, S. LeBlanc, D. Crane, H. Pangborn, C. E. Forest, A. Rattner, L. Borgsmiller, S. Priya, *Joule* **2021**, *5*, 748.
- D. Enescu, E. O. Virjoghe, *Renewable Sustainable Energy Rev.* **2014**, *38*, 903.
- X.-L. Shi, J. Zou, Z.-G. Chen, *Chem. Rev.* **2020**, *120*, 7399.
- Y. Zhang, Y. Chen, C. Gong, J. Yang, R. Qian, Y. Wang, *J. Microelectromech. Syst.* **2007**, *16*, 1113.
- I. Chowdhury, R. Prasher, K. Lofgreen, G. Chrysler, S. Narasimhan, R. Mahajan, D. Koester, R. Alley, R. Venkatasubramanian, *Nat. Nanotechnol.* **2009**, *4*, 235.
- R. Venkatasubramanian, E. Siivola, T. Colpitts, B. O'quinn, *Nature* **2001**, *413*, 597.
- G. Bulman, P. Barletta, J. Lewis, N. Baldasaro, M. Manno, A. Bar-Cohen, B. Yang, *Nat. Commun.* **2016**, *7*, 10302.
- H. Böttner, G. Chen, R. Venkatasubramanian, *MRS Bull.* **2006**, *31*, 211.
- R. Venkatasubramanian, T. Colpitts, B. O'Quinn, S. Liu, N. El-Masry, M. Lamvik, *Appl. Phys. Lett.* **1999**, *75*, 1104.
- H. Wu, X. Liu, P. Wei, H.-Y. Zhou, X. Mu, D.-Q. He, W.-T. Zhu, X.-L. Nie, W.-Y. Zhao, Q.-J. Zhang, *J. Electron. Mater.* **2017**, *46*, 2950.
- Z. Xiao, K. Hedgemen, M. Harris, E. DiMasi, *J. Vac. Sci. Technol., A* **2010**, *28*, 679.
- M. Hines, J. Lenhardt, M. Lu, L. Jiang, Z. Xiao, *J. Vac. Sci. Technol., A* **2012**, *30*, 041509.

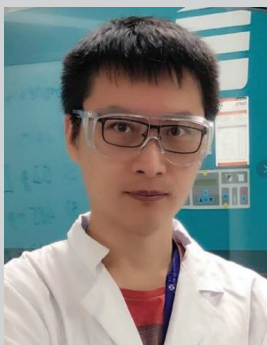
- [19] Y. Yu, W. Zhu, X. Kong, Y. Wang, P. Zhu, Y. Deng, *Front. Chem. Sci. Eng.* **2020**, *14*, 492.
- [20] W. Hou, X. Nie, W. Zhao, H. Zhou, X. Mu, W. Zhu, Q. Zhang, *Nano Energy* **2018**, *50*, 766.
- [21] X.-L. Shi, W.-Y. Chen, T. Zhang, J. Zou, Z.-G. Chen, *Energy Environ. Sci.* **2021**, *14*, 729.
- [22] T. Zhang, K. Li, J. Zhang, M. Chen, Z. Wang, S. Ma, N. Zhang, L. Wei, *Nano Energy* **2017**, *41*, 35.
- [23] W. Jin, L. Liu, T. Yang, H. Shen, J. Zhu, W. Xu, S. Li, Q. Li, L. Chi, C.-A. Di, D. Zhu, *Nat. Commun.* **2018**, *9*, 3586.
- [24] T. Cao, X.-L. Shi, J. Zou, Z.-G. Chen, *Microstructures* **2021**, *1*, 2021007.
- [25] D. Guo, Q. Sheng, X. Dou, Z. Wang, L. Xie, B. Yang, *Appl. Therm. Eng.* **2020**, *168*, 114888.
- [26] D. Zhao, G. Tan, *Energy* **2014**, *68*, 658.
- [27] M. Gillott, L. Jiang, S. Riffat, *Int. J. Energy Res.* **2010**, *34*, 776.
- [28] W.-Y. Chen, X.-L. Shi, J. Zou, Z.-G. Chen, *Nano Energy* **2020**, *81*, 105684.
- [29] L. Zhang, X.-L. Shi, Y.-L. Yang, Z.-G. Chen, *Mater. Today* **2021**, *46*, 62.
- [30] D. Zhao, X. Lu, T. Fan, Y. S. Wu, L. Lou, Q. Wang, J. Fan, R. Yang, *Appl. Energy* **2018**, *218*, 282.
- [31] R. A. Kishore, A. Nozariybar, B. Poudel, M. Sanghadasa, S. Priya, *Nat. Commun.* **2019**, *10*, 1765.
- [32] L. Lou, D. Shou, H. Park, D. Zhao, Y. S. Wu, X. Hui, R. Yang, E. C. Kan, J. Fan, *Energy Build.* **2020**, *226*, 110374.
- [33] S. Hong, Y. Gu, J. K. Seo, J. Wang, P. Liu, Y. S. Meng, S. Xu, R. Chen, *Sci. Adv.* **2019**, *5*, 0536.
- [34] J. Sharp, J. Bierschenk, H. B. Lyon, *Proc. IEEE* **2006**, *94*, 1602.
- [35] H. M. Hu, T. S. Ge, Y. J. Dai, R. Z. Wang, *Int. J. Refrig.* **2016**, *62*, 30.
- [36] Z. Xiao, X. Zhu, *Sensors* **2015**, *15*, 17232.
- [37] S. O. Tan, H. Demirel, *Comput. Electr. Eng.* **2015**, *46*, 46.
- [38] S. Wiriyasart, C. Hommalee, P. Naphon, *Case Stud. Therm. Eng.* **2019**, *14*, 100445.
- [39] X. Hao, B. Peng, G. Xie, Y. Chen, *Appl. Therm. Eng.* **2016**, *100*, 170.
- [40] S. Al-Shehri, H. H. Saber, *J. King Saud Univ., Eng. Sci.* **2020**, *32*, 321.
- [41] H. H. Saber, S. A. AlShehri, W. Maref, *Energy Convers. Manage.* **2019**, *191*, 174.
- [42] X. Lin, S. Mo, B. Mo, L. Jia, Y. Chen, Z. Cheng, *Appl. Therm. Eng.* **2020**, *172*, 115165.
- [43] X. Lin, S. Mo, L. Jia, Z. Yang, Y. Chen, Z. Cheng, *Appl. Energy* **2019**, *242*, 232.
- [44] H.-L. Tsai, P. T. Le, *Energy Convers. Manage.* **2016**, *118*, 170.
- [45] J. Li, B. Ma, R. Wang, L. Han, *Microelectron. Reliab.* **2011**, *51*, 2210.
- [46] J. Wang, J.-b. Wang, Z.-y. Long, T. Zhu, Z.-s. Li, Z.-c. Jiang, J. Liu, *Int. J. Therm. Sci.* **2021**, *162*, 106761.
- [47] Y. Lyu, A. R. M. Siddique, S. A. Gadsden, S. Mahmud, *Res. Eng.* **2021**, *10*, 100214.
- [48] S. Arora, *J. Power Sources* **2018**, *400*, 621.
- [49] J. Kim, J. Oh, H. Lee, *Appl. Therm. Eng.* **2019**, *149*, 192.
- [50] A. R. M. Siddique, S. Mahmud, B. V. Heyst, *J. Power Sources* **2018**, *401*, 224.
- [51] M. Lu, X. Zhang, J. Ji, X. Xu, Y. Zhang, *J. Energy Storage* **2020**, *27*, 101155.
- [52] T. Parashchuk, N. Sidorenko, L. Ivantsov, A. Sorokin, M. Maksymuk, B. Dzundza, Z. Dashevsky, *J. Power Sources* **2021**, *496*, 229821.
- [53] A. Çağlar, *Int. J. Refrig.* **2018**, *96*, 70.
- [54] E. Söylemez, E. Alpman, A. Onat, *Int. J. Refrig.* **2018**, *95*, 93.
- [55] D. Astrain, A. Martínez, A. Rodríguez, *Appl. Therm. Eng.* **2012**, *39*, 140.
- [56] V. P. Joshi, V. S. Joshi, H. A. Kothari, M. D. Mahajan, M. B. Chaudhari, K. D. Sant, *Energy Procedia* **2017**, *109*, 161.
- [57] M. Eslami, F. Tajeddini, N. Etaati, *Energy Convers. Manage.* **2018**, *174*, 417.
- [58] Z. Slanina, M. Uhlik, V. Sladeczek, *IFAC-PapersOnLine* **2018**, *51*, 54.
- [59] D. F. Cooke, A. B. Goldring, I. Yamayoshi, P. Tsourkas, G. H. Recanzone, A. Tiriach, T. Pan, S. I. Simon, L. Krubitzer, *J. Neurophysiol.* **2012**, *107*, 3543.
- [60] D. Wu, W. Wu, *Sensors* **2019**, *19*, 1609.
- [61] W. He, J. Zhou, J. Hou, C. Chen, J. Ji, *Appl. Energy* **2013**, *107*, 89.
- [62] T.-C. Cheng, C.-H. Cheng, Z.-Z. Huang, G.-C. Liao, *Energy* **2011**, *36*, 133.
- [63] I. Sarbu, A. Dorca, *Int. J. Energy Res.* **2018**, *42*, 395.
- [64] S. Lv, Y. Ji, Z. Qian, W. He, Z. Hu, M. Liu, *Energy* **2021**, *219*, 119625.
- [65] Z. Liu, L. Zhang, G. Gong, H. Li, G. Tang, *Energy Build.* **2015**, *102*, 207.
- [66] M. Ibañez-Puy, J. Bermejo-Busto, C. Martín-Gómez, M. Vidaurre-Arbizu, J. A. Sacristán-Fernández, *Appl. Energy* **2017**, *200*, 303.
- [67] X. Xu, S. V. Dessel, A. Messac, *Build. Environ.* **2007**, *42*, 1489.
- [68] X. Xu, S. Van Dessel, *Energy Build.* **2008**, *40*, 168.
- [69] Z. Liu, L. Zhang, G. Gong, T. Han, *Energy Convers. Manage.* **2015**, *94*, 253.
- [70] R. A. Khire, A. Messac, S. Van Dessel, *Int. J. Heat Mass. Transfer* **2005**, *48*, 4028.
- [71] C. Martín-Gómez, M. Ibañez-Puy, J. Bermejo-Busto, J. A. Sacristán Fernández, J. C. Ramos, A. Rivas, *Build. Serv. Eng. Res. Trans.* **2015**, *37*, 431.
- [72] L. Shen, X. Pu, Y. Sun, J. Chen, *Energy* **2016**, *113*, 9.
- [73] X. Su, L. Zhang, Z. Liu, Y. Luo, D. Chen, W. Li, *Renewable Energy* **2021**, *171*, 1061.
- [74] Y. Cai, W.-W. Wang, C.-W. Liu, W.-T. Ding, D. Liu, F.-Y. Zhao, *Renewable Energy* **2020**, *147*, 1565.
- [75] Q. Zhang, Z. Zhou, M. Dylla, M. T. Agne, Y. Pei, L. Wang, Y. Tang, J. Liao, J. Li, S. Bai, *Nano Energy* **2017**, *41*, 501.
- [76] V. K. Patel, K. R. Gluesenkamp, D. Goodman, A. Gehl, *Appl. Energy* **2018**, *217*, 221.
- [77] D. Zhao, G. Tan, *Appl. Therm. Eng.* **2014**, *66*, 15.
- [78] Y. Wang, L. Yang, X. Shi, X. Shi, L. Chen, M. Dargusch, J. Zou, Z.-G. Chen, *Adv. Mater.* **2019**, *31*, 1807916.
- [79] Y. Liu, Y. Su, *Appl. Therm. Eng.* **2018**, *144*, 747.
- [80] Y. Lan, A. J. Minnich, G. Chen, Z. Ren, *Adv. Funct. Mater.* **2010**, *20*, 357.
- [81] J. Ding, W. Zhao, W. Jin, C.-A. Di, D. Zhu, *Adv. Funct. Mater.* **2021**, *31*, 2010695.
- [82] S. M. Pourkiaei, M. H. Ahmadi, M. Sadeghzadeh, S. Moosavi, F. Pourfayaz, L. Chen, M. A. Pour Yazdi, R. Kumar, *Energy* **2019**, *186*, 115849.
- [83] L. Hu, H. Wu, T. Zhu, C. Fu, J. He, P. Ying, X. Zhao, *Adv. Energy Mater.* **2015**, *5*, 1500411.
- [84] S. I. Kim, K. H. Lee, H. A. Mun, H. S. Kim, S. W. Hwang, J. W. Roh, D. J. Yang, W. H. Shin, X. S. Li, Y. H. Lee, *Science* **2015**, *348*, 109.
- [85] J. Hwang, H. Kim, M.-K. Han, J. Hong, J.-H. Shim, J.-Y. Tak, Y. S. Lim, Y. Jin, J. Kim, H. Park, *ACS Nano* **2019**, *13*, 8347.
- [86] X. Chen, H. Wu, J. Cui, Y. Xiao, Y. Zhang, J. He, Y. Chen, J. Cao, W. Cai, S. J. Pennycook, *Nano Energy* **2018**, *52*, 246.
- [87] D. Yang, X. Su, J. Li, H. Bai, S. Wang, Z. Li, H. Tang, K. Tang, T. Luo, Y. Yan, J. Wu, J. Yang, Q. Zhang, C. Uher, M. G. Kanatzidis, X. Tang, *Adv. Mater.* **2020**, *32*, 2003730.
- [88] Y.-F. Tsai, P.-C. Wei, L. Chang, K.-K. Wang, C.-C. Yang, Y.-C. Lai, C.-R. Hsing, C.-M. Wei, J. He, G. J. Snyder, H.-J. Wu, *Adv. Mater.* **2020**, *33*, 2005612.
- [89] J. Yu, C. Fu, Y. Liu, K. Xia, U. Aydemir, T. C. Chasapis, G. J. Snyder, X. Zhao, T. Zhu, *Adv. Energy Mater.* **2018**, *8*, 1701313.
- [90] Y. Wu, Z. Chen, P. Nan, F. Xiong, S. Lin, X. Zhang, Y. Chen, L. Chen, B. Ge, Y. Pei, *Joule* **2019**, *3*, 1276.
- [91] G. Rogl, A. Grytsiv, K. Yubuta, S. Puchegger, E. Bauer, C. Raju, R. Mallik, P. Rogl, *Acta Mater.* **2015**, *95*, 201.
- [92] C. Zhou, Y. K. Lee, Y. Yu, S. Byun, Z.-Z. Luo, H. Lee, B. Ge, Y.-L. Lee, X. Chen, J. Y. Lee, O. Cojocar-Mirédin, H. Chang, J. Im,

- S.-P. Cho, M. Wuttig, V. P. Dravid, M. G. Kanatzidis, I. Chung, *Nat. Mater.* **2021**, 20, 1378.
- [93] Y. Gu, X.-L. Shi, L. Pan, W.-D. Liu, Q. Sun, X. Tang, L.-Z. Kou, Q. -F. Liu, Y.-F. Wang, Z.-G. Chen, *Adv. Funct. Mater.* **2021**, 31, 2101289.
- [94] M. Acharya, S. S. Jana, M. Ranjan, T. Maiti, *Nano Energy* **2021**, 84, 105905.
- [95] A. U. Khan, N. Vlachos, T. Kyratsi, *Scr. Mater.* **2013**, 69, 606.
- [96] Y. He, P. Lu, X. Shi, F. Xu, T. Zhang, G. J. Snyder, C. Uher, L. Chen, *Adv. Mater.* **2015**, 27, 3639.
- [97] M. Hong, Z. G. Chen, L. Yang, Z. M. Liao, Y. C. Zou, Y. H. Chen, S. Matsumura, J. Zou, *Adv. Energy Mater.* **2017**, 8, 1702333.
- [98] Y. Saiga, B. Du, S. Deng, K. Kajisa, T. Takabatake, *J. Alloys Compd.* **2012**, 537, 303.
- [99] B. B. Iversen, *Nat. Mater.* **2021**, 20, 1309.
- [100] S. Wiriyasart, P. Naphon, *Int. J. Heat Mass. Transfer* **2021**, 164, 120562.
- [101] N. V. Krishna, S. Manikandan, C. Selvam, *IOP Conf. Ser.: Mater. Sci. Eng.* **2021**, 1130, 012031.
- [102] B. Qin, D. Wang, X. Liu, Y. Qin, J.-F. Dong, J. Luo, J.-W. Li, W. Liu, G. Tan, X. Tang, J.-F. Li, J. He, L.-D. Zhao, *Science* **2021**, 373, 556.
- [103] R. Somdalen, J. Köhler, *Mater. Today: Proc.* **2018**, 5, 10323.
- [104] N. Ahamed, L. G. Asirvatham, S. Wongwiswes, *Exp. Therm. Fluid. Sci.* **2016**, 74, 81.
- [105] M. Z. Yilmazoglu, *Energy Build.* **2016**, 113, 51.
- [106] L. Shen, F. Xiao, H. Chen, S. Wang, *Energy Build.* **2013**, 59, 123.
- [107] W.-S. Liu, Q. Zhang, Y. Lan, S. Chen, X. Yan, Q. Zhang, H. Wang, D. Wang, G. Chen, Z. Ren, *Adv. Energy Mater.* **2011**, 1, 577.
- [108] M. Cosnier, G. Fraise, L. Luo, *Int. J. Refrig.* **2008**, 31, 1051.
- [109] Z. Lu, M. Layani, X. Zhao, L. P. Tan, T. Sun, S. Fan, Q. Yan, S. Magdassi, H. H. Hng, *Small* **2014**, 10, 3551.
- [110] I. Y. Huang, J.-C. Lin, K.-D. She, M.-C. Li, J.-H. Chen, J.-S. Kuo, *Sens. Actuators, A* **2008**, 148, 176.
- [111] L. M. Goncalves, J. G. Rocha, C. Couto, P. Alpuim, G. Min, D. M. Rowe, J. H. Correia, *J. Micromech. Microeng.* **2007**, 17, S168.
- [112] L. W. de Silva, M. Kaviani, *J. Microelectromech. Syst.* **2005**, 14, 1110.
- [113] G. J. Snyder, J. R. Lim, C.-K. Huang, J.-P. Fleurial, *Nat. Mater.* **2003**, 2, 528.
- [114] G. E. Bulman, E. Siivola, B. Shen, R. Venkatasubramanian, *Appl. Phys. Lett.* **2006**, 89, 122117.
- [115] A. Shakouri, Z. Yan, *IEEE Trans. Compon., Packag., Technol.* **2005**, 28, 65.
- [116] W. He, G. Zhang, X. Zhang, J. Ji, G. Li, X. Zhao, *Appl. Energy* **2015**, 143, 1.
- [117] E. S. Jeong, *Cryogenics* **2014**, 59, 38.
- [118] B. David, J. Ramousse, L. Luo, *Energy Convers. Manage.* **2012**, 60, 125.
- [119] S. Palaniappan, B. Palanisamy, *Procedia Eng.* **2013**, 64, 1056.
- [120] Y.-X. Huang, X.-D. Wang, C.-H. Cheng, D. T.-W. Lin, *Energy* **2013**, 59, 689.
- [121] S. Sharma, V. K. Dwivedi, S. N. Pandit, *Int. J. Green Energy* **2014**, 11, 899.
- [122] R. He, G. Schierning, K. Nielsch, *Adv. Mater. Technol.* **2018**, 3, 1700256.
- [123] S. B. Riffat, X. Ma, *Appl. Therm. Eng.* **2003**, 23, 913.
- [124] M. K. Rawat, H. Chattopadhyay, S. Neogi, *Int. J. Emergy Technol. Adv. Eng.* **2013**, 3, 362.
- [125] S. B. Riffat, X. Ma, *Int. J. Energy Res.* **2004**, 28, 753.
- [126] S. Twaha, J. Zhu, Y. Yan, B. Li, *Renewable Sustainable Energy Rev.* **2016**, 65, 698.
- [127] R. Chein, G. Huang, *Appl. Therm. Eng.* **2004**, 24, 2207.
- [128] R. Gouws, H. Eilers, *Sci. Res. Essays* **2013**, 8, 485.
- [129] S. Khode, P. Kale, C. Gandhile, *Int. J. Eng. Tech. Res.* **2015**, 3, 71.
- [130] S. Baru, S. Bhatia, *IOP Conf. Ser.: Mater. Sci. Eng.* **2020**, 912, 042004.
- [131] M. Dargusch, W.-D. Liu, Z.-G. Chen, *Adv. Sci.* **2020**, 7, 2001362.
- [132] S. H. Zaferani, M. W. Sams, R. Ghomashchi, Z.-G. Chen, *Nano Energy* **2021**, 90, 106572.
- [133] Y. Du, J. Xu, B. Paul, P. Eklund, *Appl. Mater. Today* **2018**, 12, 366.
- [134] S. Fan, J. Zhao, J. Guo, Q. Yan, J. Ma, H. H. Hng, *Appl. Phys. Lett.* **2010**, 96, 182104.
- [135] C. -J. Liu, H.-C. Lai, Y.-L. Liu, L.-R. Chen, *J. Mater. Chem.* **2012**, 22, 4825.
- [136] M. Hong, Z.-G. Chen, J. Zou, *Chin. Phys. B* **2018**, 27, 048403.
- [137] L. Hu, T. Zhu, X. Liu, X. Zhao, *Adv. Funct. Mater.* **2014**, 24, 5211.
- [138] L. D. Zhao, B. P. Zhang, J. F. Li, H. L. Zhang, W. S. Liu, *Solid State Sci.* **2008**, 10, 651.
- [139] H. Choi, K. Jeong, J. Chae, H. Park, J. Baek, T. H. Kim, J. Y. Song, J. Park, K.-H. Jeong, M.-H. Cho, *Nano Energy* **2018**, 47, 374.
- [140] M. Tan, W. D. Liu, X. L. Shi, H. Gao, H. Li, C. Li, X. B. Liu, Y. Deng, Z. G. Chen, *Small Methods* **2019**, 3, 1900582.
- [141] J. A. Perez-Taborda, O. Caballero-Calero, L. Vera-Londono, F. Briones, M. Martin-Gonzalez, *Adv. Energy Mater.* **2018**, 8, 1702024.
- [142] M. Tan, L. Hao, H. Li, C. Li, X. Liu, D. Yan, T. Yang, Y. Deng, *Sci. Rep.* **2020**, 10, 5978.
- [143] M. Tan, W.-D. Liu, X.-L. Shi, J. Shang, H. Li, X. Liu, L. Kou, M. Dargusch, Y. Deng, Z.-G. Chen, *Nano Energy* **2020**, 78, 105379.
- [144] J. Chen, H. Chen, F. Hao, X. Ke, N. Chen, T. Yajima, Y. Jiang, X. Shi, K. Zhou, M. Döbeli, T. Zhang, B. Ge, H. Dong, H. Zeng, W. Wu, L. Chen, *ACS Energy Lett.* **2017**, 2, 915.
- [145] T. Harman, P. Taylor, M. Walsh, B. LaForge, *Science* **2002**, 297, 2229.
- [146] J. Zhang, T. Zhang, H. Zhang, Z. Wang, C. Li, Z. Wang, K. Li, X. Huang, M. Chen, Z. Chen, Z. Tian, H. Chen, L.-D. Zhao, L. Wei, *Adv. Mater.* **2020**, 32, 2002702.
- [147] J.-H. Meng, X.-D. Wang, X.-X. Zhang, *Appl. Energy* **2013**, 108, 340.
- [148] Z.-G. Chen, X. Shi, L.-D. Zhao, J. Zou, *Prog. Mater. Sci.* **2018**, 97, 283.
- [149] G. Lee, C. S. Kim, S. Kim, Y. J. Kim, H. Choi, B. J. Cho, *Energy* **2019**, 179, 12.
- [150] H. Lim, Y.-K. Kang, J.-W. Jeong, *Appl. Therm. Eng.* **2018**, 144, 248.
- [151] Y. Shi, Y. Wang, D. Mei, Z. Chen, *IEEE Access* **2018**, 6, 43602.
- [152] J. Choi, C. Dun, C. Forsythe, M. P. Gordon, J. J. Urban, *J. Mater. Chem. A* **2021**, 9, 15696.
- [153] H. Lv, X.-D. Wang, T.-H. Wang, C.-H. Cheng, *Appl. Energy* **2016**, 164, 501.
- [154] D. K. Aswal, R. Basu, A. Singh, *Energy Convers. Manage.* **2016**, 114, 50.
- [155] P. Ziolkowski, P. Blaschkewitz, E. Müller, *Measurement* **2021**, 177, 109247.
- [156] M. Tan, X.-L. Shi, W.-D. Liu, M. Li, Y. Wang, H. Li, Y. Deng, Z.-G. Chen, *Adv. Energy Mater.* **2021**, 11, 2102578.
- [157] L. Fu, K. H. Lee, S.-I. Kim, J.-H. Lim, W. Choi, Y. Cheng, M.-W. Oh, Y.-M. Kim, S. W. Kim, *Acta Mater.* **2021**, 215, 117058.
- [158] G. Yang, L. Sang, D. R. G. Mitchell, F. Fei Yun, K. Wai See, A. Jumlat Ahmed, S. Sayyar, A. Bake, P. Liu, L. Chen, Z. Yue, D. Cortie, X. Wang, *Chem. Eng. J.* **2022**, 428, 131205.
- [159] B. Y. Yavorsky, N. F. Hinsche, I. Mertig, P. Zahn, *Phys. Rev. B* **2011**, 84, 165208.
- [160] Y. Wang, W. Liu, H. Gao, L. Wang, M. Li, X.-L. Shi, M. Hong, H. Wang, J. Zou, Z.-G. Chen, *ACS Appl. Mater. Interfaces* **2019**, 11, 31237.
- [161] H. Qin, Y. Liu, Z. Zhang, Y. Wang, J. Cao, W. Cai, Q. Zhang, J. Sui, *Mater. Today Phys.* **2018**, 6, 31.
- [162] Y. Wang, W.-D. Liu, X.-L. Shi, M. Hong, L.-J. Wang, M. Li, H. Wang, J. Zou, Z.-G. Chen, *Chem. Eng. J.* **2019**, 391, 123513.
- [163] Y. Wang, M. Hong, W.-D. Liu, X.-L. Shi, S.-D. Xu, Q. Sun, H. Gao, S. Lu, J. Zou, Z.-G. Chen, *Chem. Eng. J.* **2020**, 397, 125360.

- [164] T. Day, F. Drymiotis, T. Zhang, D. Rhodes, X. Shi, L. Chen, G. J. Snyder, *J. Mater. Chem. C* **2013**, 1, 7568.
- [165] F. F. Aliev, M. B. Jafarov, V. I. Eminova, *Semiconductors+* **2009**, 43, 977.
- [166] M. Ferhat, J. Nagao, *J. Appl. Phys.* **2000**, 88, 813.
- [167] B. Qin, D. Wang, W. He, Y. Zhang, H. Wu, S. J. Pennycook, L.-D. Zhao, *J. Am. Chem. Soc.* **2018**, 141, 1141.
- [168] L.-D. Zhao, G. Tan, S. Hao, J. He, Y. Pei, H. Chi, H. Wang, S. Gong, H. Xu, V. P. Dravid, *Science* **2016**, 351, 141.
- [169] K. Peng, B. Zhang, H. Wu, X. Cao, A. Li, D. Yang, X. Lu, G. Wang, X. Han, C. Uher, *Mater. Today* **2018**, 21, 501.
- [170] X.-L. Shi, X. Tao, J. Zou, Z.-G. Chen, *Adv. Sci.* **2020**, 7, 1902923.
- [171] L.-D. Zhao, C. Chang, G. Tan, M. G. Kanatzidis, *Energy Environ. Sci.* **2016**, 9, 3044.
- [172] X.-L. Shi, W.-Y. Chen, X. Tao, J. Zou, Z.-G. Chen, *Mater. Horiz.* **2020**, 7, 3065.
- [173] C. Chang, G. Tan, J. He, M. G. Kanatzidis, L.-D. Zhao, *Chem. Mater.* **2018**, 30, 7355.
- [174] S. D. Yang, R. K. Nutor, Z. J. Chen, H. Zheng, H. F. Wu, J. X. Si, *J. Electron. Mater.* **2017**, 46, 6662.
- [175] X. Shi, Z.-G. Chen, W. Liu, L. Yang, M. Hong, R. Moshwan, L. Huang, J. Zou, *Energy Storage Mater.* **2018**, 10, 130.
- [176] M. Jin, X.-L. Shi, T. Feng, W. Liu, H. Feng, S. T. Pantelides, J. Jiang, Y. Chen, Y. Du, J. Zou, Z.-G. Chen, *ACS Appl. Mater. Interfaces* **2019**, 11, 8051.
- [177] X. Shi, A. Wu, W. Liu, R. Moshwan, Y. Wang, Z.-G. Chen, J. Zou, *ACS Nano* **2018**, 12, 11417.
- [178] L. D. Zhao, S. H. Lo, Y. Zhang, H. Sun, G. Tan, C. Uher, C. Wolverton, V. P. Dravid, M. G. Kanatzidis, *Nature* **2014**, 508, 373.
- [179] X. L. Shi, K. Zheng, M. Hong, W. D. Liu, R. Moshwan, Y. Wang, X.-L. Qu, Z. G. Chen, J. Zou, *Chem. Sci.* **2018**, 9, 7376.
- [180] X. Shi, A. Wu, T. Feng, K. Zheng, W. Liu, Q. Sun, M. Hong, S. T. Pantelides, Z. G. Chen, J. Zou, *Adv. Energy Mater.* **2019**, 9, 1803242.
- [181] X.-L. Shi, W.-D. Liu, A.-Y. Wu, V. T. Nguyen, H. Gao, Q. Sun, R. Moshwan, J. Zou, Z.-G. Chen, *InfoMat* **2020**, 2, 1201.
- [182] C. Chang, M. Wu, D. He, Y. Pei, C.-F. Wu, X. Wu, H. Yu, F. Zhu, K. Wang, Y. Chen, *Science* **2018**, 360, 778.
- [183] X. L. Shi, K. Zheng, W. D. Liu, Y. Wang, Y. Z. Yang, Z. G. Chen, J. Zou, *Adv. Energy Mater.* **2018**, 8, 1800775.
- [184] L. Su, T. Hong, D. Wang, S. Wang, B. Qin, M. Zhang, X. Gao, C. Chang, L.-D. Zhao, *Mater. Today Phys.* **2021**, 20, 100452.
- [185] Y.-X. Chen, X.-L. Shi, Z.-H. Zheng, F. Li, W.-D. Liu, W.-Y. Chen, X.-R. Li, G.-X. Liang, J.-T. Luo, P. Fan, Z.-G. Chen, *Mater. Today Phys.* **2021**, 16, 100306.
- [186] M. Hong, K. Zheng, W. Lyv, M. Li, X. Qu, Q. Sun, S. Xu, J. Zou, Z.-G. Chen, *Energy Environ. Sci.* **2020**, 13, 1856.
- [187] S. Xu, M. Hong, X.-L. Shi, Y. Wang, L. Ge, Y. Bai, L. Wang, M. Dargusch, J. Zou, Z.-G. Chen, *Chem. Mater.* **2019**, 31, 5238.
- [188] S. Xu, M. Hong, X.-L. Shi, M. Li, Q. Sun, Q. Chen, M. Dargusch, J. Zou, Z.-G. Chen, *Energy Environ. Sci.* **2020**, 13, 3480.
- [189] S. Anwar, S. Gowthamaraju, B. K. Mishra, S. K. Singh, A. Shahid, *Mater. Chem. Phys.* **2015**, 153, 236.
- [190] M. M. Rashid, K. H. Cho, G.-S. Chung, *Appl. Surf. Sci.* **2013**, 279, 23.
- [191] X. Gong, M. Feng, H. Wu, H. Zhou, C. Suen, H. Zou, L. Guo, K. Zhou, S. Chen, J. Dai, G. Wang, X. Zhou, *Appl. Surf. Sci.* **2021**, 535, 147694.
- [192] D. Zhao, J. Chen, Z. Ren, J. Chen, Q. Song, Q. Zhang, N. Chen, Y. Jiang, *Ceram. Int.* **2020**, 46, 3339.
- [193] Z.-H. Zheng, X.-L. Shi, D.-W. Ao, W.-D. Liu, Y.-X. Chen, F. Li, S. Chen, X.-Q. Tian, X.-R. Li, J.-Y. Duan, H.-L. Ma, X.-H. Zhang, G.-X. Liang, P. Fan, Z.-G. Chen, *Nano Energy* **2021**, 81, 105683.
- [194] Z.-H. Zheng, J.-Y. Niu, D.-W. Ao, B. Jabar, X.-L. Shi, X.-R. Li, F. Li, G.-X. Liang, Y.-X. Chen, Z.-G. Chen, P. Fan, *J. Mater. Sci. Technol.* **2021**, 92, 178.
- [195] T. Parashchuk, O. Kostyuk, L. Nykyruy, Z. Dashevsky, *Mater. Chem. Phys.* **2020**, 253, 123427.
- [196] M. E. DeCoster, X. Chen, K. Zhang, C. M. Rost, E. R. Hoglund, J. M. Howe, T. E. Beechem, H. Baumgart, P. E. Hopkins, *Adv. Funct. Mater.* **2019**, 29, 1904073.
- [197] J. P. Singh, R. K. Bedi, *J. Appl. Phys.* **1990**, 68, 2776.
- [198] S. Hou, Y. Liu, L. Yin, C. Chen, Z. Wu, J. Wang, Y. Luo, W. Xue, X. Liu, Q. Zhang, F. Cao, *Nano Energy* **2021**, 87, 106223.
- [199] B. Subramanian, C. Sanjeeviraja, M. Jayachandran, *J. Cryst. Growth* **2002**, 234, 421.
- [200] Z. Zainal, N. Saravanan, K. Anuar, M. Z. Hussein, W. M. M. Yunus, *Mater. Sci. Eng., B* **2004**, 107, 181.
- [201] S. Xu, X.-L. Shi, M. Dargusch, C. Di, J. Zou, Z.-G. Chen, *Prog. Mater. Sci.* **2021**, 121, 100840.
- [202] E. J. X. Pang, S. J. Pickering, A. Chan, K. H. Wong, P. L. Lau, *J. Solid State Chem.* **2012**, 193, 147.
- [203] J. Choi, Y. Jung, S. J. Yang, J. Y. Oh, J. Oh, K. Jo, J. G. Son, S. E. Moon, C. R. Park, H. Kim, *ACS Nano* **2017**, 11, 7608.
- [204] A. Morata, M. Pacios, G. Gadea, C. Flox, D. Cadavid, A. Cabot, A. Tarancón, *Nat. Commun.* **2018**, 9, 4759.
- [205] F. Ma, Y. Ou, Y. Yang, Y. Liu, S. Xie, J.-F. Li, G. Cao, R. Proksch, J. Li, *J. Phys. Chem. C* **2010**, 114, 22038.
- [206] X.-L. Shi, H. Wu, Q. Liu, W. Zhou, S. Lu, Z. Shao, M. Dargusch, Z.-G. Chen, *Nano Energy* **2020**, 78, 105195.
- [207] D. Liang, H. Yang, S. W. Finefrock, Y. Wu, *Nano Lett.* **2012**, 12, 2140.
- [208] L. Ruan, Y. Zhao, Z. Chen, W. Zeng, S. Wang, D. Liang, J. Zhao, *Polymers* **2020**, 12, 553.
- [209] Y. Zheng, Q. Zhang, W. Jin, Y. Jing, X. Chen, X. Han, Q. Bao, Y. Liu, X. Wang, S. Wang, Y. Qiu, C.-a. Di, K. Zhang, *J. Mater. Chem. A* **2020**, 8, 2984.
- [210] Y. Zheng, X.-L. Shi, H. Yuan, S. Lu, X. Qu, W. Liu, L. Wang, K. Zheng, J. Zou, Z.-G. Chen, *Mater. Today Phys.* **2020**, 13, 100198.
- [211] X. Fan, G. Zeng, C. LaBounty, J. E. Bowers, E. Croke, C. C. Ahn, S. Huxtable, A. Majumdar, A. Shakouri, *Appl. Phys. Lett.* **2001**, 78, 1580.
- [212] X. Li, C. Xie, S. Quan, L. Huang, W. Fang, *Appl. Energy* **2018**, 231, 887.
- [213] K. Irshad, A. Almalawi, A. I. Khan, M. M. Alam, M. H. Zahir, A. Ali, *Sustainability* **2020**, 12, 1564.
- [214] H. Imoto, M. Fujii, J. Uchiyama, H. Fujisawa, K. Nakano, I. Kunitsugu, S. Nomura, T. Saito, M. Suzuki, *J. Neurosurg.* **2006**, 104, 150.
- [215] R. Hu, Y. Liu, S. Shin, S. Huang, X. Ren, W. Shu, J. Cheng, G. Tao, W. Xu, R. Chen, X. Luo, *Adv. Energy Mater.* **2020**, 10, 1903921.
- [216] P. Qiu, T. Mao, Z. Huang, X. Xia, J. Liao, M. T. Agne, M. Gu, Q. Zhang, D. Ren, S. Bai, *Joule* **2019**, 3, 1538.
- [217] F. Rajaei, M. A. V. Rad, A. Kasaieian, O. Mahian, W.-M. Yan, *Energy Convers. Manage.* **2020**, 212, 112780.
- [218] Y. Su, J. Lu, D. Villaroman, D. Li, B. Huang, *Nano Energy* **2018**, 48, 202.



Wen-Yi Chen received his master's degree from the University of Queensland in 2020. He is a Ph.D. candidate at the University of Queensland. His current research focuses on thermoelectric materials and devices targeting cooling applications under the supervision of Prof. Zhi-Gang Chen and Dr. Xiao-Lei Shi.



Xiao-Lei Shi currently works at the University of Southern Queensland. He received his Ph.D. degree in 2019 from the University of Queensland under the supervision of Prof. Jin Zou and Prof. Zhi-Gang Chen with a research focus on the development of high-performance thermoelectrics and underlying physics and chemistry.



Jin Zou is currently an Emeritus Professor at the University of Queensland. He received his Ph.D. in materials physics in late 1993 from Sydney University, Australia, and worked there for 10 years with various prestigious fellowships, including an Australian Government's Queen Elizabeth II Fellowship. In the second half of 2003, he moved to the University of Queensland and continued his research in the field of semiconductor nanostructures for energy-related applications.



Zhi-Gang Chen is currently a professor of energy materials in the University of Southern Queensland (USQ). He received his Ph.D. in materials science and engineering from the Institute of Metal Research, Chinese Academy of Science, in 2008. After his Ph.D., he worked at the University of Queensland for seven years before moving to USQ in 2016. His research concentrates on smart functional materials for thermoelectrics and nanoelectronics from synthesizing materials to understanding their underlying physics and chemistry.